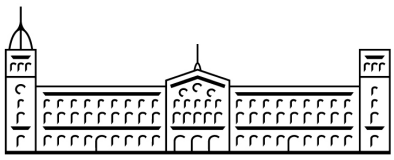

Undergraduate Thesis

DEGREE IN MATHEMATICS

Faculty of Mathematics and Informatics
Universitat de Barcelona

Invariant manifolds associated to periodic orbits around Mars

Author: David Capilla Guilarte

Director:	**Dr. Gerard Gómez Muntané**
Department:	**Applied Mathematics and Analysis.**
Barcelona,	**June 29, 2017**

Contents

The main purpose of this work is to explore if it is possible to find a transfer trajectory from the vicinity of the Earth to Mars that uses the stable invariant manifolds associated to some families of periodic orbits around Mars. This means that the study in a theoretic level of both periodic orbits and invariant manifolds is in the roadmap.

The study of the Solar System is complex because of the interaction between all the planets and the Sun, however, there are some simplifications that can be done. Due to our interest in the study of spacecraft periodic orbits around Mars it is adopted the approach of a three-body problem, considering only the Sun, Mars and an artificial satellite.

There has been extensively research in the field throughout the years and although the two-body problem is a well-known problem with well-known solutions, the three-body problem is neither solved nor is the behaviour of the dynamical system completely understood. It has to be said that whereas the two-body problem is completely integrable, the three body problem is not. The restricted three-body problem is of special interest because of its application in celestial mechanics, stellar dynamics or space mechanics.

Due to the fact that the objective is to apply these theoretic aspects to the restricted three-body problem with Sun and Mars as primaries, the necessary software, using the C++ language, has to be developed in order to compute the desired objects and run the simulations.

This work is organised in the following way: In chapter 1 it is introduced the planar circular restricted three-body problem, which describes the framework of our problem. The problem is formulated in dimensionless coordinates and its Hamiltonian is constructed. Chapter 2 is mainly divided in two parts, one related to periodic orbits and another to invariant manifolds. In the first part, devoted to periodic orbits, it is seen the CR3BP as a perturbation of the Hill's problem, that allows us to use circular Keplerian orbits of the two body problem as a good approximation of periodic orbits of the CR3BP around Mars. Then, it is exposed the necessary theory in order to show that the orbits are grouped in families, that concludes with the Cylinder Theorem. Finally, this first part ends explaining the numerical methods used to continue the orbits along the family. The second part briefly exposes the theory of invariant manifolds and its application to periodic orbits. In chapter 3, there is a more detailed implementation of the methods and there are exposed the results of the computations. The work ends with some conclusions and future work.

Although most of the proofs of theorems or propositions are broadly found in bibliography, in this work it has been opted for redo most of this demonstrations in order to gain a better insight of the theory.

Chapter 1

The planar circular restricted three-body problem

In this chapter is introduced the three-body problem under some restrictions, it is formulated in terms of dimensionless coordinates and finally its Hamiltonian is constructed. References to this problem can be found in [1], [2] and [3].

1.1 Definition

The three-body problem is a classical mathematical problem that describes the motion of three point masses m_1, m_2 and m_3, that interact with each other by means of its gravitational attraction. In the so called restricted three body problem one of the bodies is much less massive than the other two $(m_3 << m_1, m_2)$ and therefore its gravitational influence over them is negligible. The main problem that we will consider is the planar and circular restricted three body problem (CR3BP), in which the two massive bodies move around the center of mass of the system in circular orbits and the third body moves only in the same plane these two do.

So for this problem, we have two masses m_1 and m_2 revolving around the center of mass following circular orbits, and therefore, in an inertial reference system with origin at the center of mass of m_1 and m_2, the coordinates for these two objects are:

$$\begin{cases} x_1^c(\tau) = -R_1\cos(\omega\tau), & y_1^c(\tau) = -R_1\sin(\omega\tau), \\ x_2^c(\tau) = R_2\cos(\omega\tau), & y_2^c(\tau) = R_2\sin(\omega\tau), \end{cases} \tag{1.1}$$

where the super-index c denotes that are Cartesian inertial coordinates, ω is the constant mean motion of m_1 and m_2, and τ denotes time.

As we are considering an inertial reference frame, the Newton's second law provide the equation of motion for the m_3 mass:

$$\sum \vec{F}^c = \frac{d}{d\tau}(\vec{p}^c) = m_3\frac{d^2\boldsymbol{X}^c}{d\tau}, \tag{1.2}$$

where $\boldsymbol{X}^c = (x_3^c, y_3^c)^T$ is the position of m_3, $\vec{\boldsymbol{p}}^c$ its linear momentum, and $\vec{\boldsymbol{F}}^c$ are the forces acting on m_3[1]. On the other hand, the forces acting over m_3 are due to the Newton's law of universal gravitation, and thus

$$\boldsymbol{F}_{i3}^c = -G\frac{m_i m_3}{(r_{i3}^c)^3}\boldsymbol{r}_{i3}^c\,, \tag{1.3}$$

where $\boldsymbol{r}_{i3}^c$ are the position vectors that point from the mass m_i to m_3 for $i \in \{1,2\}$ and G is the universal gravitational constant. From now on we will use $\boldsymbol{r}_i^c$ instead of $\boldsymbol{r}_{i3}^c$ and omit the sub-index referent to the mass m_3, whenever no confusion is possible. Then, as $\boldsymbol{r}_i^c = \boldsymbol{X}^c - \boldsymbol{X}_i^c$ we have:

$$\boldsymbol{r}_1^c(\tau) = \begin{pmatrix} x^c + R_1\cos(\omega\tau) \\ y^c + R_1\sin(\omega\tau) \end{pmatrix}, \qquad \boldsymbol{r}_2^c(\tau) = \begin{pmatrix} x^c - R_2\cos(\omega\tau) \\ y^c - R_2\sin(\omega\tau) \end{pmatrix}. \tag{1.4}$$

So the dynamical system will be driven by the following differential equation:

$$\frac{d^2\boldsymbol{X}^c}{d\tau^2} = -G\left(\frac{m_1}{(r_1^c)^3}\boldsymbol{r}_1^c + \frac{m_2}{(r_2^c)^3}\boldsymbol{r}_2^c\right). \tag{1.5}$$

1.2 Formulation in the rotating system

In order to simplify the formulation, and remove the time dependence of the right hand side of the equations of motion, it is convenient to introduced a rotating reference frame, in which the two primaries (m_1 and m_2) are fixed. This change of variables is given by $\boldsymbol{X}^* = \mathcal{R}\boldsymbol{X}^c$, where $\mathcal{R}$ is the rotation matrix

$$\mathcal{R} = \begin{pmatrix} \cos(\omega\tau) & \sin(\omega\tau) \\ -\sin(\omega\tau) & \cos(\omega\tau) \end{pmatrix}. \tag{1.6}$$

The inverse transformation is $\boldsymbol{X}^c = \mathcal{R}^{-1}\boldsymbol{X}^* = \mathcal{R}^T\boldsymbol{X}^*$ and, therefore, the differential equation becomes

$$\frac{d^2\boldsymbol{X}^c}{d\tau^2} = \frac{d}{d\tau}\left(\frac{d\mathcal{R}^T}{d\tau}\boldsymbol{X}^* + \mathcal{R}^T\frac{d\boldsymbol{X}^*}{d\tau}\right) = \frac{d^2\mathcal{R}^T}{d\tau^2}\boldsymbol{X}^* + 2\frac{d\mathcal{R}^T}{d\tau}\frac{d\boldsymbol{X}^*}{d\tau} + \mathcal{R}^T\frac{d^2\boldsymbol{X}^*}{d\tau^2}. \tag{1.7}$$

As

$$\frac{d\mathcal{R}^T}{d\tau} = \begin{pmatrix} -\omega\sin(\omega\tau) & -\omega\cos(\omega\tau) \\ \omega\cos(\omega\tau) & -\omega\sin(\omega\tau) \end{pmatrix} = \omega\mathcal{R}^T A, \tag{1.8}$$

where

$$A = \begin{pmatrix} 0 & -1 \\ 1 & 0 \end{pmatrix},$$

we get

$$\frac{d^2\mathcal{R}^T}{d\tau^2} = \frac{d}{d\tau}\left(\frac{d\mathcal{R}^T}{d\tau}\right) = \omega\frac{d\mathcal{R}^T}{d\tau}A = \omega^2\mathcal{R}^T A^2 = -\omega^2\mathcal{R}^T. \tag{1.9}$$

[1]Notation: The bold symbols will denote vectorial variables whereas non-bold symbols will denote scalar variables.

Since $A^2 = -Id$, we can write

$$\frac{d^2\boldsymbol{X}^c}{d\tau^2} = \frac{\boldsymbol{F}^c_{tot}}{m_3} = \boldsymbol{f}^c_{tot} = \mathcal{R}^T \boldsymbol{f}^*_{tot} = -\omega^2 \mathcal{R}^T \boldsymbol{X}^* + 2\omega \mathcal{R}^T A \frac{d\boldsymbol{X}^*}{d\tau} + \mathcal{R}^T \frac{d^2\boldsymbol{X}^*}{d\tau^2}, \tag{1.10}$$

or

$$\boldsymbol{f}^*_{tot} = \frac{d^2\boldsymbol{X}^*}{d\tau^2} + 2\omega A \frac{d\boldsymbol{X}^*}{d\tau} - \omega^2 \boldsymbol{X}^*, \tag{1.11}$$

or , equivalently

$$\begin{cases} \dfrac{d^2x^*}{d\tau^2} - 2\omega \dfrac{dy^*}{d\tau} = \dfrac{\partial \mathcal{F}}{\partial x^*}\,, \\ \dfrac{d^2y^*}{d\tau^2} + 2\omega \dfrac{dx^*}{d\tau} = \dfrac{\partial \mathcal{F}}{\partial y^*}\,, \end{cases} \tag{1.12}$$

where $\mathcal{F}$ is a potential such that

$$\begin{cases} \dfrac{\partial \mathcal{F}}{\partial x^*} = \omega^2 x^* - G\left(m_1 \dfrac{x^* + R_1}{(r_1^*)^3} + m_2 \dfrac{x^* - R_2}{(r_2^*)^3} \right), \\ \dfrac{\partial \mathcal{F}}{\partial y^*} = \omega^2 y^* - G\left(m_1 \dfrac{y^*}{(r_1^*)^3} + m_2 \dfrac{y^*}{(r_2^*)^3} \right). \end{cases} \tag{1.13}$$

In order to find the potential $\mathcal{F}$, we can use that

$$\mathcal{F} = \int \frac{\partial \mathcal{F}}{\partial y^*} dy^* + \varphi(x^*) =$$

$$= \frac{\omega^2 (y^*)^2}{2} - G\left(m_1 \int \frac{y^*}{((x^* + R_1)^2 + (y^*)^2)^{\frac{3}{2}}} + m_2 \int \frac{y^*}{((x^* - R_2)^2 + (y^*)^2)^{\frac{3}{2}}} \right) + \varphi(x^*) =$$

$$= \frac{\omega^2 (y^*)^2}{2} + G\left(\frac{m_1}{((x^* + R_1)^2 + (y^*)^2)^{\frac{1}{2}}} + \frac{m_2}{((x^* - R_2)^2 + (y^*)^2)^{\frac{1}{2}}} \right) + \varphi(x^*),$$

and then

$$\frac{\partial \mathcal{F}}{\partial x^*} = -G\left(m_1 \frac{x^* + R_1}{(r_1^*)^3} + m_2 \frac{x^* - R_2}{(r_2^*)^3} \right) + \frac{\partial \varphi(x^*)}{\partial x^*} \overset{Eq.(1.13)}{\Longrightarrow}$$

$$\Rightarrow \frac{\partial \varphi(x^*)}{\partial x^*} = \omega^2 x^* \Rightarrow \varphi(x^*) = \frac{\omega^2 (x^*)^2}{2} + C.$$

So we end up with

$$\mathcal{F} = \frac{1}{2}\omega^2 \left((x^*)^2 + (y^*)^2 \right) + G\left(\frac{m_1}{r_1^*} + \frac{m_2}{r_2^*} \right) + C. \tag{1.14}$$

1.3 Dimensionless coordinates

The following scaling of variables is usually done in order to use dimensionless coordinates and units

$$x = \frac{x^*}{\ell}, \quad y = \frac{y^*}{\ell}, \quad t = \omega\tau, \quad \mu_1 = \frac{m_1}{M}, \quad \mu_2 = \frac{m_2}{M},$$

where $\ell = r_{12} = R_1 + R_2$ and $M = m_1 + m_2$.

Expressing Eq. (1.12) in the dimensionless coordinates, we get

$$\begin{cases} \omega^2\ell\ddot{x} - 2\omega^2\ell\dot{y} = \dfrac{1}{\ell}\dfrac{\partial\mathcal{F}}{\partial x}, \\ \\ \omega^2\ell\ddot{y} + 2\omega^2\ell\dot{x} = \dfrac{1}{\ell}\dfrac{\partial\mathcal{F}}{\partial y}, \end{cases} \tag{1.15}$$

with $\mathcal{F}(x,y) = \dfrac{1}{2}\omega^2(\ell^2x^2 + \ell^2y^2) + G\left(\dfrac{m_1}{\ell r_1} + \dfrac{m_2}{\ell r_2}\right) + C$. Since C is an arbitrary constant, it can be taken as $C = \dfrac{\omega^2 l^2}{2}\dfrac{m_1m_2}{(m_1+m_2)^2}$, and then

$$\mathcal{F}(x,y) = \frac{1}{2}\omega^2\ell^2(x^2+y^2) + \frac{Gm_1}{\ell}\frac{1}{r_1} + \frac{Gm_2}{\ell}\frac{1}{r_2} + \frac{\omega^2 l^2}{2}\mu_1\mu_2. \tag{1.16}$$

Using the fact that the gravity force acts as a centripetal force, i.e. $G\dfrac{m_1m_2}{r_{12}} = m_1\omega^2R_1 = m_2\omega^2R_2$, we can write

$$\frac{Gm_1}{\ell} = \omega^2\ell R_2 \quad \text{and} \quad \frac{Gm_2}{\ell} = \omega^2\ell R_1.$$

Moreover, adding both expressions leads to

$$G\frac{m_1+m_2}{\ell} = G\frac{M}{\ell} = \omega^2\ell(R_1+R_2) = \omega^2\ell^2, \tag{1.17}$$

and dividing the above two expressions by this last one we obtain $\mu_1 = \dfrac{R_2}{\ell}$ and $\mu_2 = \dfrac{R_1}{\ell}$. Then, the potential can be expressed as

$$\mathcal{F}(x,y) = \omega^2\ell^2\left(\frac{1}{2}(x^2+y^2) + \frac{\mu_1}{r_1} + \frac{\mu_2}{r_2} + \frac{1}{2}\mu_1\mu_2\right), \tag{1.18}$$

from which it follows

$$\begin{cases} \ddot{x} - 2\dot{y} = \dfrac{1}{\omega^2\ell^2}\dfrac{\partial\mathcal{F}}{\partial x} = \dfrac{\partial\Omega}{\partial x}, \\ \\ \ddot{y} + 2\dot{x} = \dfrac{1}{\omega^2\ell^2}\dfrac{\partial\mathcal{F}}{\partial y} = \dfrac{\partial\Omega}{\partial y}, \end{cases} \tag{1.19}$$

where $\Omega = \dfrac{\mathcal{F}}{\omega^2\ell^2} = \dfrac{x^2+y^2}{2} + \dfrac{\mu_1}{r_1} + \dfrac{\mu_2}{r_2} + \dfrac{\mu_1\mu_2}{2}$. As $r_1^2 = (x+\mu_2)^2 + y^2 = x^2 + 2x\mu_2 + \mu_2^2 + y^2$ and $r_2^2 = (x-\mu_1)^2 + y^2 = x^2 - 2x\mu_1 + \mu_1^2 + y^2$ then

$$\mu_1r_1^2 + \mu_2r_2^2 = \overbrace{(\mu_1+\mu_2)}^{1}x^2 + \mu_1\mu_2^2 + \mu_1^2\mu_2 + \overbrace{(\mu_1+\mu_2)}^{1}y^2 =$$

$$= x^2 + y^2 + \mu_1\mu_2(\mu_1 + \mu_2) = x^2 + y^2 + \mu_1\mu_2.$$

Using that $\mu_1 + \mu_2 = \dfrac{m_1}{m_1+m_2} + \dfrac{m_2}{m_1+m_2} = 1$, we see that the model depends on only one parameter. Then, defining $\mu \equiv \mu_2$ we have $\mu_1 = 1 - \mu$ and finally the differential equations of the model can be expressed as

$$\begin{cases} \ddot{x} - 2\dot{y} = \Omega_x, \\ \ddot{y} + 2\dot{x} = \Omega_y, \end{cases} \tag{1.20}$$

with $\Omega_x \equiv \dfrac{\partial \Omega}{\partial x}$ and $\Omega_y \equiv \dfrac{\partial \Omega}{\partial y}$ where

$$\Omega = \frac{1}{2}\left((1-\mu)r_1^3 + \mu r_2^3\right) + \frac{1-\mu}{r_1} + \frac{\mu}{r_2}. \tag{1.21}$$

It is useful to express (1.20) as a system of first order differential equations, $\dot{\boldsymbol{X}} = \boldsymbol{f}(\boldsymbol{X})$, where $\boldsymbol{X} = (x, y, \dot{x}, \dot{y})^T = (x_1, x_2, x_3, x_4)^T$, so the differential equations of the CR3BP become

$$f(\boldsymbol{X}) = \begin{pmatrix} \dot{x} \\ \dot{y} \\ 2\dot{y} + \Omega_x \\ -2\dot{x} + \Omega_y \end{pmatrix} = \begin{pmatrix} x_3 \\ x_4 \\ 2x_4 + \left(1 - \dfrac{1}{r_1^3}\right)(x_1 + \mu)(1-\mu) + \left(1 - \dfrac{1}{r_2^3}\right)(x_1 + \mu - 1)\mu \\ -2x_3 + \left(1 - \dfrac{1}{r_1^3}\right)x_2(1-\mu) + \left(1 - \dfrac{1}{r_2^3}\right)x_2\mu \end{pmatrix}. \tag{1.22}$$

1.4 Jacobian integral

Multiplying the first equation in (1.20) by $\dot{x}$, the second by $\dot{y}$ and adding them up we obtain

$$\ddot{x}\dot{x} + \ddot{y}\dot{y} = \Omega_x\dot{x} + \Omega_y\dot{y},$$

which is equivalent to write

$$\frac{1}{2}\frac{d}{dt}\left(\dot{x}^2 + \dot{y}^2\right) = \frac{d\Omega}{dt}.$$

Integrating the above expression, we get

$$\frac{1}{2}(\dot{x}^2 + \dot{y}^2) = \Omega - C, \tag{1.23}$$

where C is an arbitrary constant. This equation is a first integral of (1.20) and is usually known as the Jacobian integral. We will use it to test the numerical integration of the equations of motion.

The so-called *zero velocity curves* can be obtained from the Jacobian integral setting $\dot{x} = \dot{y} = 0$. These curves are defined by

$$F = \Omega - C = \frac{1}{2}\left((1-\mu)r_1^2 + \mu r_2^2\right) + \frac{1-\mu}{r_1} + \frac{\mu}{r_2} - C = 0, \tag{1.24}$$

and delimit the regions in the configuration space (positions) that are not accessible for the m_3, since this would imply that $\dot{x}^2 + \dot{y}^2 < 0$.

1.5 Hamiltonian of the problem

In this section we briefly construct the Hamiltonian of the planar circular restricted three-body problem. In the inertial reference frame, we can write the kinetic and potential energies as

$$T = \frac{m_3}{2}\left[\left(\frac{dx^c}{d\tau}\right)^2 + \left(\frac{dy^c}{d\tau}\right)^2\right] \quad \text{and} \quad V = -m_3\left(\frac{Gm_1}{r_1^c} + \frac{Gm_2}{r_2^c}\right). \tag{1.25}$$

Since $x^c = \ell(\cos(\omega\tau)x - \sin(\omega\tau)y)$ and $y^c = \ell(\sin(\omega\tau)x + \cos(\omega\tau)y)$, then

$$\begin{aligned}\frac{dx^c}{d\tau} &= \omega\ell(-\sin(\omega\tau)x + \cos(\omega\tau)\dot{x} - \cos(\omega\tau)y - \sin(\omega\tau)\dot{y}) = \\ &= \omega\ell((\dot{x} - y)\cos(\omega\tau) - (\dot{y} + x)\sin(\omega\tau)),\end{aligned}$$

and

$$\begin{aligned}\frac{dy^c}{d\tau} &= \omega\ell(\cos(\omega\tau)x + \sin(\omega\tau)\dot{x} - \sin(\omega\tau)y + \cos(\omega\tau)\dot{y}) = \\ &= \omega\ell((\dot{x} - y)\sin(\omega\tau) + (\dot{y} + x)\cos(\omega\tau)),\end{aligned}$$

so, we can write T as

$$T = \frac{m_3\omega^2\ell^2}{2}\left[(\dot{x} - y)^2 + (\dot{y} + x)^2\right]. \tag{1.26}$$

For the potential V, we have

$$V = -m_3\omega^2\ell^2\left(\frac{R_2}{\ell r_1} + \frac{R_1}{\ell r_2}\right) = -m_3\omega^2\ell^2\left(\frac{1-\mu}{r_1} + \frac{\mu}{r_2}\right), \tag{1.27}$$

and defining $q_1 = x$, $q_2 = y$, the Lagrangian becomes

$$\mathcal{L}(\boldsymbol{q}, \dot{\boldsymbol{q}}, t) = T - V = m_3\omega^2\ell^2\left\{\frac{1}{2}\left[(\dot{x} - y)^2 + (\dot{y} + x)^2\right] + \left(\frac{1-\mu}{r_1} + \frac{\mu}{r_2}\right)\right\}. \tag{1.28}$$

According to the definition of the momenta $\tilde{p}_i = \dfrac{\partial\mathcal{L}}{\partial\dot{q}_i}$, we have

$$\tilde{p}_1 = \frac{\partial\mathcal{L}}{\partial\dot{q}_1} = m_3\omega^2\ell^2(\dot{x} - y) \quad \text{and} \quad \tilde{p}_2 = \frac{\partial\mathcal{L}}{\partial\dot{q}_2} = m_3\omega^2\ell^2(\dot{y} + x),$$

so

$$\dot{x} = \frac{\tilde{p}_1}{m_3\omega^2\ell^2} + y \quad \text{and} \quad \dot{y} = \frac{\tilde{p}_2}{m_3\omega^2\ell^2} - x,$$

therefore, the Hamiltonian $\tilde{\mathcal{H}}$ will be

$$\tilde{\mathcal{H}} = \sum_i \dot{q}_i\tilde{p}_i - \mathcal{L} = \frac{1}{2m_3\omega^2\ell^2}(\tilde{p}_1^2 + \tilde{p}_2^2) + y\tilde{p}_1 - x\tilde{p}_2 - m_3\omega^2\ell^2\left(\frac{1-\mu}{r_1} + \frac{\mu}{r_2}\right).$$

Defining $p_x = \dfrac{\tilde{p}_1}{m_3\omega^2\ell^2}$, $p_y = \dfrac{\tilde{p}_2}{m_3\omega^2\ell^2}$ and $\mathcal{H} = \dfrac{\tilde{\mathcal{H}}}{m_3\omega^2\ell^2}$, we get

$$\mathcal{H} = \frac{1}{2}(p_x^2 + p_y^2) + yp_x - xp_y - \frac{1-\mu}{r_1} - \frac{\mu}{r_2}, \tag{1.29}$$

and, as usual, the equations of motion are given by

$$\dot{q}_i = \frac{\partial \mathcal{H}}{\partial p_i} \quad \text{and} \quad \dot{p}_i = -\frac{\partial \mathcal{H}}{\partial q_i}. \tag{1.30}$$

Chapter 2

Periodic orbits, invariant manifolds and its numerical computation

The main purpose of this chapter is to explain the numerical methods that have been used for the computation of families of periodic orbits of the CR3BP, as well as their stable/unstable manifolds. We have also included the theoretical framework and results required for the explanations.

The chapter is divided in two main sections, one devoted to the computation of periodic orbits and and one to the computation of invariant manifolds. In the first section we explain the continuation method, that allows the numerical computation of families of periodic orbits, and that is based on the implicit function theorem. It is also introduced a refinement method of the obtained orbit in terms of a modified Newton method. In the second section it is introduced the notion of stable and unstable manifold and some of its properties. The results and their demonstrations of periodic orbits can be found in [1], [2], [3] and [4]. In addition to those, there have been used in the part of the invariant manifolds [5], [6] and [7]. Finally the algorithms can be found in [8] and [9].

2.1 Periodic orbits

We are interested in periodic orbits around the small mass m_2 of the dynamical system defined by (1.22). In particular, in the continuation of the circular Keplerian orbits of the two body problem to the CR3BP. There are two kinds of these orbits, the direct and retrograde ones, depending on their direction of motion around the primary. Those orbits have the particularity that are symmetrical with respect to the x-axis and, as it can be easily seen, they satisfy $\dot{x} = 0$ when crossing the $y = 0$ plane. They are also simple, in the sense of crossing the x-axis only twice during one period. This property, however, does not hold along the whole family. Both properties will be used in the computation of the families of periodic orbits in which we are interested.

The first thing to do is to show that it is possible to continue periodic orbits from circular Keplerian orbits of the two body problem to the circular restricted three body problem.

2.1.1 The CR3BP as a perturbation of Hill's problem

It seems intuitive to think that the circular Keplerian orbits of the two body problem are a good approximation of periodic orbits around the small mass of the CR3BP, at least as long as we stay close to the primary. This is because if we stay close enough to one of the primaries the influence of the other might be negligible and the problem is reduced to determine a trajectory of a massless particle moving in the gravitational field of the primary. This approximation, after some scaling of variables, defines what is called Hill's problem.

In order to demonstrate this heuristic reasoning we will see that the Hamiltonian associated to the problem, when the particle is really close to one of the primaries, tends to the Hamiltonian of the two body problem.

Let's move one of the primaries to the origin, i.e. make the change of variables $x \mapsto x' - \mu$, $y \mapsto y'$, $p_x \mapsto p'_x$ and $p_y \mapsto p'_y - \mu$. Then, the Hamiltonian defined by Eq. (1.29) becomes

$$\mathcal{H}' = \frac{1}{2}((p'_x)^2 + (p'_y)^2 - 2p'_y\mu + \mu^2) + y'p'_x - (x' - \mu)(p'_y - \mu) - \frac{1-\mu}{r'_1} - \frac{\mu}{r'_2} =$$

$$= \frac{1}{2}((p'_x)^2 + (p'_y)^2) + y'p'_x - x'p'_y - \frac{1-\mu}{\sqrt{(x')^2 + (y')^2}} - \frac{\mu}{\sqrt{(x'+1)^2 + (y')^2}} + x'\mu - \frac{\mu^2}{2}.$$

Performing the change of variables $(x', y') \mapsto (\epsilon^2 u, \epsilon^2 v)$ and $(p'_x, p'_y) \mapsto (\epsilon^{-1} p_u, \epsilon^{-1} p_v)$, we get

$$\mathcal{H}'' = \frac{1}{\epsilon^2}\left[\frac{1}{2}(p_u^2 + p_v^2) - \frac{1-\mu}{\sqrt{u^2+v^2}}\right] + \epsilon(vp_u - up_v) - \frac{\mu}{\sqrt{(\epsilon^2 u + 1)^2 + (\epsilon^2 v)^2}} + \epsilon^2 u\mu - \frac{\mu^2}{2}.$$

Multiplying the Hamiltonian by ϵ^2 and dropping the constant terms (that do not affect the equations of motion) we end up with

$$\mathcal{H}''' = \left[\frac{1}{2}(p_u^2 + p_v^2) - \frac{1-\mu}{\sqrt{u^2+v^2}}\right] + \epsilon^3(vp_u - up_v) + \mathcal{O}(\epsilon^4),$$

where

$$\frac{\epsilon^2\mu}{\sqrt{(\epsilon^2 u + 1)^2 + (\epsilon^2 v)^2}} = \epsilon^2\mu\left(1 - \epsilon^2 u + \mathcal{O}(\epsilon^4)\right) = \mu\left(\epsilon^2 + \mathcal{O}(\epsilon^4)\right),$$

which is a constant plus something of the order of ϵ^4 or more. It must be said that ϵ is a small parameter that measures the distance between the infinitesimal mass m_3 and the primary at the origin.

It can be seen that the dominant term of the above Hamiltonian is the Hamiltonian of Kepler's problem. Using polar coordinates $r = \sqrt{u^2+v^2}$, $\theta = \arctan(v/u)$, and rescaling

time ($t \mapsto \epsilon^{-3}t$), we can write

$$\dot{r} = \frac{1}{r}(u\epsilon^3\dot{u} + v\epsilon^3\dot{v}) = \frac{1}{r}(up_u + vp_v),$$

$$\dot{\theta} = \frac{1}{1+\left(\frac{v}{2}\right)^2}\left(\frac{\epsilon^3\dot{v}}{u} - \frac{v}{u^2}\epsilon^3\dot{u}\right) = \frac{1}{r^2}\left(up_v - vp_u\right) - \epsilon^3.$$

Defining $R = \dot{r}$ and $\Theta = (up_v - vp_u)$ as the momentum of the two body problem and as $p_u^2 + p_v^2 = R^2 + \frac{\Theta^2}{r^2}$, we have

$$\mathcal{H}_{polar} = \frac{1}{2}\left(R^2 + \frac{\Theta^2}{r^2}\right) - \frac{1-\mu}{r} - \epsilon^3\Theta + \mathcal{O}(\epsilon^4). \tag{2.1}$$

Using Eq (1.30) and neglecting terms of order greater than ϵ^3, we obtain

$$\dot{R} = \frac{\Theta}{r^3} + \frac{1-\mu}{r^2} \quad \text{and} \quad \dot{\Theta} = 0,$$

therefore Θ is an integral of motion. There exist two periodic solutions $\Theta = \pm(1-\mu)$, $r \equiv 1$ of period $2\pi/(1-\mu \mp \epsilon^3)$. The linearised radial equation has solutions of the form $\exp(\pm i(1-\mu)t)$, therefore, after a period the eigenvalue will be

$$\exp\left(\frac{\pm 2\pi i(1-\mu)}{1-\mu\mp\epsilon^3}\right) = \exp\left(\pm 2\pi i \frac{1}{1\mp\frac{\epsilon^3}{(1-\mu)}}\right) = \exp\left(\pm 2\pi i\left[1 \pm \frac{\epsilon^3}{1-\mu} + \mathcal{O}(\epsilon^6)\right]\right) =$$

$$= \exp\left(\pm 2\pi i\right)\exp\left(2\pi i\frac{\epsilon^3}{1-\mu}\right)\exp\left(\mathcal{O}(\epsilon^6)\right) = 1 + \frac{2\pi i}{1-\mu}\epsilon^3 + \mathcal{O}(\epsilon^6).$$

If now we considered the period map in the level surface of the Hamiltonian (which is nothing else than the Poincaré map restricted to an energy level, as it will be formally defined in Definition 2.8) about this circular orbit, then the period map is the identity up to terms of ϵ^2. The period map can be expressed as $P(s) = s + \epsilon^3 p(s) + \mathcal{O}(\epsilon^4)$, where s is the coordinate in the surface, being zero for the circular periodic orbit. As we want to obtain solutions to $(P - Id)(s) = 0$ near zero, we will apply the implicit function theorem to $G(s,\epsilon) = \frac{P-s}{\epsilon^3} = p(s) + \mathcal{O}(\epsilon)$ at $(s,\epsilon) = (0,0)$. We have that $G(0,0) = 0$ and $\frac{\partial G}{\partial s}|_{(0,0)} = \frac{\partial p}{\partial s}|_{(0)} = \frac{2\pi i}{1-\mu} \neq 0$, therefore, there exist a neighbourhood N and a function $g(\epsilon) = s$ such that $G(g(\epsilon),\epsilon) = 0\ \forall \epsilon \in N$, that is, the solutions can be continued from the circular Keplerian orbits to the CR3BP as we wanted to show.

2.1.2 Families of orbits

The aim of this section then is to show that the periodic orbits of the CR3BP are grouped in one-parametric families, and also to give a method for its computation. In this

way, once we have a periodic orbit of our problem, it is possible to obtain the orbits of the family in which it is embedded by means of the continuation procedure.

Consider a differential system $\dot{\boldsymbol{X}} = \boldsymbol{f}(\boldsymbol{X}, \mu)$ such that

$$\begin{array}{rccc} \boldsymbol{f}: & \mathcal{U} \times I \subseteq \mathbb{R}^{n+1} & \longrightarrow & \mathbb{R}^n \\ & (\boldsymbol{X}, \mu) & \longmapsto & \boldsymbol{f}(\boldsymbol{X}, \mu) \end{array} \tag{2.2}$$

and a solution of it $\boldsymbol{\varphi}(t, \boldsymbol{\xi}, \mu)$, with initial conditions $\boldsymbol{\xi}$. We will assume the mass parameter μ is constant and, therefore, it will be not explicitly written.

Now consider $\boldsymbol{\xi}^*$ such that $\boldsymbol{\varphi}(t_0, \boldsymbol{\xi}^*)$ is a periodic solution, $\boldsymbol{\varphi}(t_0, \boldsymbol{\xi}^*) = \boldsymbol{\varphi}(t_0 + \tau^*, \boldsymbol{\xi}^*) = \boldsymbol{\xi}^*$ with period τ^*. In what follows the function $\boldsymbol{f}$ is required to be differentiable with respect to $\boldsymbol{X}$. Moreover, it will be assumed that the solution it is not an equilibrium point. For the sake of simplicity, and since the differential equations are autonomous, we will suppose that $t_0 = 0$, therefore, the periodic orbit satisfies the following equation

$$\boldsymbol{F}(\tau, \boldsymbol{\xi}) = \boldsymbol{\varphi}(\tau, \boldsymbol{\xi}) - \boldsymbol{\xi} = \boldsymbol{0}$$

for $\tau = \tau^*$, $\boldsymbol{\xi} = \boldsymbol{\xi}^*$.

Using the fact that we already have one periodic solution for $\boldsymbol{\xi}^*$, we want to obtain new periodic orbits close to this one.

Variational equations

We will start with a comment about how the solution changes with time when varying the initial conditions. These changes are given by the variational equations. As long as t and $\boldsymbol{\xi}$ are independent variables

$$\frac{d}{dt}\left(\frac{\partial \varphi_i(t, \boldsymbol{\xi})}{\partial \xi_j}\right) = \frac{\partial}{\partial \xi_j}\frac{d\varphi_i(t, \boldsymbol{\xi})}{dt} = \frac{\partial}{\partial \xi_j} f_i(\boldsymbol{\varphi}(t, \boldsymbol{\xi})) = \frac{\partial f_i}{\partial x_j}(\boldsymbol{\varphi}(t, \boldsymbol{\xi})) \sum_k \frac{\partial \varphi_k}{\partial \xi_j}(t, \boldsymbol{\xi}),^1$$

or, in matrix form

$$\dot{A} = D\boldsymbol{f}(\boldsymbol{\varphi}(t, \boldsymbol{\xi}))A, \tag{2.3}$$

where $A = \left(\frac{\partial \varphi_i(t,\boldsymbol{\xi})}{\partial \xi_j}\right)$. Since $\boldsymbol{\varphi}(0, \boldsymbol{\xi}) = \boldsymbol{\xi}$, the differential equation (2.3) satisfies initial conditions $A(0) = Id$.

If we have a periodic solution of period τ, then $A(\tau)$ is denoted by M and it is called the monodromy matrix.

Uniparametric families of orbits

First of all, we will see that the monodromy matrix M is degenerated, i.e. has eigenvalues (multipliers) equal to $+1$.

[1] The sub-index will denote the component of the vector referring to that sub-index unless it is indicated the opposite.

Lemma 2.1. *Periodic solutions of (2.2) are never isolated, and $+1$ is always a multiplier. In fact, $f(\xi^*)$ is an eigenvector of the monodromy matrix corresponding to the eigenvalue $+1$*

Proof. This is due to the fact that if we consider another initial condition ξ that is on the same solution curve, it can be expressed as $\xi = \varphi(t', \xi^*)$ for a suitable t'. As the system is autonomous, we will be able to write

$$\varphi(t + t', \xi^*) = \varphi(t, \varphi(t', \xi^*)) = \varphi(t, \xi).$$

Which means that any translate of the solution is a solution and therefore the periodic solution is not isolated. Differentiating both sides with respect t' we obtain

$$\frac{d}{dt'}(\varphi(t + t', \xi^*)) = f(\varphi(t + t', \xi^*)) = f(\varphi(t, \xi))$$

for the left side and

$$\frac{d}{dt'}\varphi(t, \xi) = D_\xi \varphi(t, \xi)\frac{d}{dt'}\xi = D_\xi \varphi(t, \xi)\frac{d}{dt'}\varphi(t', \xi) = D_\xi \varphi(t, \xi) f(\xi)$$

for the right hand side, so

$$f(\varphi(t, \xi)) = D_\xi \varphi(t, \xi) f(\xi) = A(t) f(\xi). \tag{2.4}$$

Therefore, choosing $t = \tau^*$, and since $\varphi(\tau^*, \xi) = \xi$, we get that

$$f(\varphi(\tau^*, \xi)) = f(\xi) = A(\tau^*) f(\xi).$$

Since $f(\xi) \neq \mathbf{0}$ because ξ is not an equilibrium point, we conclude that $f(\xi)$ is an eigenvalue of value $+1$ of the monodromy matrix $A(\tau^*, \xi)$. By choosing $t' = 0$ it is obtained the desired proof. □

Corollary 2.2. *The determinant of the differential of the function defining the periodic orbit,*

$$D_\xi \mathbf{F}(\tau, \xi, \mu) = D_\xi \varphi(\tau, \xi, \mu) - D_\xi \xi = A(\tau) - Id,$$

is zero.

Next we will see how to avoid this degeneration. Before we give a definition and recall the flowbox theorem.

Definition 2.3. *Let $f : \mathcal{U} \subseteq \mathbb{R}^n \longrightarrow \mathbb{R}$ be a vector field, and $\gamma : \mathcal{B} \subseteq \mathbb{R}^{n-1} \longrightarrow \mathcal{U}$ an embedding defining the surface $\Sigma = \gamma(\mathcal{B})$. It is said that Σ is transverse to f if $\forall s \in \mathcal{B}$ it is satisfied that:*

$$\det\left(f(\gamma(s)) | D\gamma(s)\right) \neq 0.$$

Theorem 2.4 (The flowbox theorem)**.** *Let $r \in \mathcal{U} \subseteq \mathbb{R}^n$ be an ordinary point for $\dot{x} = f(x)$ ($f(r) \neq 0$), then there exists a change of coordinates $z = h(x)$ defined near r such that in the new coordinates $\dot{x} = f(x)$ define a parallel flow, i.e.*

$$\dot{z}_1 = 0, \ \ldots \ , \ \dot{z}_{n-1} = 0, \ \dot{z}_n = 1.$$

Although this theorem is a classical result found in many references, as for example in [2], [5] and [6], they were found difficult to follow and we decided to prove it in a different way, based in the notes of the subject of differential equations.

Proof. Let Σ be a transverse surface to $\boldsymbol{f}$, such that $\boldsymbol{\gamma}(\mathbf{0}) = \boldsymbol{r}$. Given the function

$$\begin{array}{rccl} \boldsymbol{E}: & \mathcal{U} \times I_{T,\epsilon_1} \times \mathcal{B} & \longrightarrow & \mathbb{R}^n \\ & (\boldsymbol{x}, t, \boldsymbol{s}) & \longmapsto & \boldsymbol{E}(\boldsymbol{x}, t, \boldsymbol{s}) = \boldsymbol{\varphi}(t, \boldsymbol{x}) - \boldsymbol{\gamma}(\boldsymbol{s}), \end{array}$$

we know that exists at least one solution of the equation $\boldsymbol{E} = \mathbf{0}$, since if it is taken $\boldsymbol{x_1} = \boldsymbol{\varphi}(-T, \boldsymbol{r})$, for a certain T, then $\boldsymbol{\varphi}(T, \boldsymbol{x_1}) = \boldsymbol{r}$ and the equation has solution for the values $\boldsymbol{x} = \boldsymbol{x_1}$, $t = T$ and $\boldsymbol{s} = \mathbf{0}$. As

$$\det\left(\frac{\partial \boldsymbol{E}}{\partial t}(\boldsymbol{x_1}, T, \mathbf{0}) | D_{\boldsymbol{s}}\boldsymbol{E}(\boldsymbol{x_1}, T, \mathbf{0})\right) = \det\left(\boldsymbol{f}(\boldsymbol{r}) | - D_{\boldsymbol{s}}\boldsymbol{\gamma}(\mathbf{0})\right) \neq 0,$$

by the transversality condition, then it is possible to apply the implicit function theorem so $\exists \mathcal{V} \subseteq \mathcal{U}, \exists \epsilon \leq \epsilon_1, \exists \mathcal{B}_0 \subseteq \mathcal{B}$ such that $\boldsymbol{r} \in \mathcal{V}, \mathbf{0} \in \mathcal{B}_0$ and

$$\begin{array}{rccl} \exists(\tau, \boldsymbol{\sigma}): & \mathcal{V} & \longrightarrow & I_{T,\epsilon} \times \mathcal{B}_0 \\ & \boldsymbol{x} & \longmapsto & (\tau(\boldsymbol{x}), \boldsymbol{\sigma}(\boldsymbol{x}))^T, \end{array}$$

satisfying $\boldsymbol{E}(\boldsymbol{x}, \tau(\boldsymbol{x}), \boldsymbol{\sigma}(\boldsymbol{x})) = 0$ or $\boldsymbol{\varphi}(\tau(\boldsymbol{x}), \boldsymbol{x}) = \boldsymbol{\gamma}(\boldsymbol{\sigma}(\boldsymbol{x}))$. Then, the differential of the function given by the implicit function theorem is

$$\begin{pmatrix} D\tau(\boldsymbol{x}) \\ D\boldsymbol{\sigma}(\boldsymbol{x}) \end{pmatrix} = -\left(\boldsymbol{f}(\boldsymbol{\varphi}(\tau(\boldsymbol{x}), \boldsymbol{x})) | - D_{\boldsymbol{s}}\boldsymbol{\gamma}(\boldsymbol{\sigma}(\boldsymbol{x}))\right)^{-1} D_{\boldsymbol{x}}\boldsymbol{\varphi}(\tau(\boldsymbol{x}), \boldsymbol{x}).$$

Considering now

$$\begin{array}{rccl} \boldsymbol{h}: & \mathcal{V} & \longrightarrow & I_{0,\epsilon} \times \mathcal{B}_0 \\ & \boldsymbol{x} & \longmapsto & (-\tau(\boldsymbol{x}), \boldsymbol{\sigma}(\boldsymbol{x}))^T, \end{array}$$

it can be seen that

$$\begin{aligned} D\boldsymbol{h}(\boldsymbol{x})\boldsymbol{f}(\boldsymbol{x}) &= \left(\boldsymbol{f}(\boldsymbol{\varphi}(\tau(\boldsymbol{x}), \boldsymbol{x})) | D_{\boldsymbol{s}}\boldsymbol{\gamma}(\boldsymbol{\sigma}(\boldsymbol{x}))\right)^{-1} D_{\boldsymbol{x}}\boldsymbol{\varphi}(\tau(\boldsymbol{x}), \boldsymbol{x})\boldsymbol{f}(\boldsymbol{x}) \overset{Eq.(2.4)}{=} \\ &= \left(\boldsymbol{f}(\boldsymbol{\varphi}(\tau(\boldsymbol{x}), \boldsymbol{x})) | D_{\boldsymbol{s}}\boldsymbol{\gamma}(\boldsymbol{\sigma}(\boldsymbol{x}))\right)^{-1} \boldsymbol{f}(\boldsymbol{\varphi}(\tau(\boldsymbol{x}), \boldsymbol{x})) = (1, 0, ..., 0)^T. \end{aligned}$$

Therefore, if $\boldsymbol{z} = \boldsymbol{h}(\boldsymbol{x})$ then $\dot{\boldsymbol{z}} = \dfrac{d}{dt}\boldsymbol{h}(\boldsymbol{x}) = D\boldsymbol{h}(\boldsymbol{x})\boldsymbol{f}(\boldsymbol{x}) = (1, 0, ..., 0)^T$. By a redefinition of the coordinates we will have the desired change of variables.

□

Lemma 2.5. *If the multipliers of the periodic solution are $1, \lambda_2, ..., \lambda_n$, then the multipliers of the corresponding fixed point of the Poincaré map are $\lambda_2, ..., \lambda_n$.*

Proof. By theorem 2.4, there are coordinates $\boldsymbol{z}$ such that, after a translation of the origin of coordinates, Σ is defined by $z_n = 0$. As $\boldsymbol{f}(z_0) = f(z_0)\hat{z}_n$ then $M(z_0) = D_{\boldsymbol{z}}\boldsymbol{\varphi}(\tau, z_0)$. The monodromy matrix in these coordinates will be

$$M(\boldsymbol{z}_0) = \begin{pmatrix} & & & 0 \\ & M' & & \vdots \\ & & & 0 \\ X & \cdots & X & 1 \end{pmatrix}.$$

Then, the eigenvalues corresponding to M', associated with the Poincaré map, will be $\lambda_2, ..., \lambda_n$.

□

Let us see that if the problem has a non-degenerate first integral, then multiplicity of the eigenvalue $+1$ of the monodromy matrix M is greater than 1.

Lemma 2.6. *If C is a non-degenerate integral on the periodic solution $\boldsymbol{\varphi}(t, \boldsymbol{\xi})$, then the multiplier +1 has algebraic multiplicity at least 2. Moreover, the row vector $D_{\boldsymbol{\xi}}C$ is a left eigenvector of the monodromy matrix corresponding to the eigenvalue +1.*

Proof. It has been seen in Lemma 2.1 that the monodromy matrix has already $\boldsymbol{f}(\boldsymbol{\xi}^*)$ as eigenvector of eigenvalue of value $+1$, then it has to be seen that $D_{\boldsymbol{\xi}}C$ is an eigenvector of the monodromy matrix corresponding to the eigenvalue $+1$.

If the system has a non-degenerate integral $C = C(\boldsymbol{X})$ then it satisfies

$$0 = \frac{dC}{dt} = D_{\boldsymbol{X}}C(\boldsymbol{X})\frac{d}{dt}\boldsymbol{X}(t) = D_{\boldsymbol{X}}C(\boldsymbol{X})\boldsymbol{f}(\boldsymbol{X}). \tag{2.5}$$

Under the assumption of $D_{\boldsymbol{X}}C \neq \boldsymbol{0}$, as $\boldsymbol{f}(\boldsymbol{\xi}^*) \neq \boldsymbol{0}$ then it must be a component of $D_{\boldsymbol{X}}C$ different from the n-th that is different from zero, let's suppose that component is the $(n-1)$-th.

As C is constant along the solution, $C(\boldsymbol{\varphi}(t, \boldsymbol{\xi})) = C(\boldsymbol{\xi})$, then

$$D_{\boldsymbol{X}}C(\boldsymbol{\varphi}(t, \boldsymbol{\xi}))D_{\boldsymbol{\xi}}\boldsymbol{\varphi}(t, \boldsymbol{\xi}) = D_{\boldsymbol{X}}C(\boldsymbol{\xi}) \Rightarrow D_{\boldsymbol{X}}C(\boldsymbol{\xi}^*)A(\tau^*, \boldsymbol{\xi}^*) = D_{\boldsymbol{X}}C(\boldsymbol{\xi}^*).$$

That means that $D_{\boldsymbol{X}}C(\boldsymbol{\xi}^*)$ is a left eigenvector of the monodromy matrix $M = A(\tau^*, \boldsymbol{\xi}^*)$ of eigenvalue $+1$.

□

In order to avoid this new degeneracy, it is convenient to introduce the Poincaré map in an integral surface and use the following theorem.

Theorem 2.7. *If $\dot{\boldsymbol{x}} = \boldsymbol{f}(\boldsymbol{x})$ admits a non-degenerate integral C at $r \in \mathcal{U}$, where r is an ordinary point, then the flow box given in Theorem 2.4 can be chosen so that $C(\boldsymbol{z}) = z_{n-1}$.*

Proof. Let $\boldsymbol{z}$ be the coordinate system given by Theorem 2.4. As C is a first integral, C is independent of z_n (this is because the flow will be $\psi(t, \boldsymbol{z}) = (z_1, ..., z_{n-1}, z_n + t)$). Then, as C is non-degenerated it follows that for some $i \in \{1, ..., n-1\}$ it is satisfied that $\dfrac{\partial C}{\partial z_i}(\boldsymbol{r}) \neq 0$,

let's say for $i = n-1$. Making the change of variables $z'_j = z_j$ for $j \in \{1, ..., n-2\}$ and $z'_{n-1} = C(z_1, ..., z_{n-1})$ defined by $\boldsymbol{h}(z_1, ..., z_{n-1})$, as

$$D\boldsymbol{h}(z_1, ..., z_{n-1}) = \begin{pmatrix} & & & 0 \\ & Id & & \vdots \\ & & & 0 \\ 0 & \cdots & 0 & \dfrac{\partial C}{\partial z_{n-1}} \end{pmatrix},$$

so, $\det\left(D\boldsymbol{h}(z_1, ..., z_{n-1})\right) \neq 0$ and by the inverse function theorem it defines a change of coordinates in a neighbourhood of $\boldsymbol{r}$.

□

Consider the Poincaré map $\boldsymbol{P} : N \longrightarrow \Sigma$, where N is a neighbourhood of $\boldsymbol{w}$ in Σ. Let $\boldsymbol{z}$ be a local coordinate system at $\boldsymbol{w}$ such that $\boldsymbol{w}$ corresponds to $\boldsymbol{z} = \boldsymbol{0}$ and, according to Theorem 2.4, $\dot{\boldsymbol{X}} = \boldsymbol{f}(\boldsymbol{X})$ in these coordinates becomes $\dot{z}_1 = 0, ..., \dot{z}_{n-1} = 0, \dot{z}_n = 1$ at $\boldsymbol{w}$. Moreover, according to Theorem 2.7, we have taken the first integral $C(\boldsymbol{z}) = z_{n-1}$. Defining Σ by $\xi_n = 0$, since ξ_{n-1} is the first integral in these coordinates, $\boldsymbol{P}$ maps the level sets $\xi_{n-1} = cte$ into themselves, so we can ignore the ξ_{n-1} component of $\boldsymbol{P}$.

Now, let $e = \xi_{n-1}$ and Σ_e the intersection of Σ and the level set $C = e$, then $\bar{\boldsymbol{\xi}} \equiv (\xi_1, ..., \xi_{n-2})$ will be the coordinates in Σ_e. In what follows e will be considered as a parameter, and in these coordinates $\boldsymbol{P} = \boldsymbol{P}(\bar{\boldsymbol{\xi}}, e)$.

Definition 2.8. *The Poincaré map in an integral surface is defined by the map*

$$\begin{array}{rccc} \boldsymbol{Q}(\cdot, e): & N_e \subseteq \Sigma_e & \longrightarrow & \Sigma_e \\ & \bar{\boldsymbol{\xi}} & \longmapsto & \boldsymbol{Q}(\bar{\boldsymbol{\xi}}, e) \end{array}$$

that satisfies $\boldsymbol{P}(\bar{\boldsymbol{\xi}}, e) = \big(\boldsymbol{Q}(\bar{\boldsymbol{\xi}}, e), e\big)$*, and where* N_e *is a neighbourhood of the origin in* Σ_e*.*

Lemma 2.9. *If the multipliers of the periodic solution of a system with non-degenerate integral are* $1, 1, \lambda_3, ..., \lambda_n$*, then the multipliers of the fixed point in the of the Poincaré map in the integral surface are* $\lambda_3, ..., \lambda_n$*.*

Proof. In the coordinates previously defined, we have that the monodromy matrix is

$$M(\boldsymbol{z}_0) = \begin{pmatrix} & & & X & 0 \\ & M'' & & \vdots & \vdots \\ & & & X & 0 \\ 0 & \cdots & 0 & 1 & 0 \\ X & \cdots & X & X & 1 \end{pmatrix},$$

being M'' the associated with the Poincaré map in the integral.

□

The next theorem states that an elementary orbit for a system with an integral is not isolated and that in fact the orbit lays in a one-parameter family of orbits.

Theorem 2.10 (The cylinder theorem)**.** *An elementary periodic orbit ($\lambda_3, ..., \lambda_n \neq 1$) of a system with an integral lies in a smooth cylinder of periodic solutions parametrized by the integral C.*

Proof. Let $\bar{\boldsymbol{\xi}}^*$ be a fixed point of the Poincaré map in the integral surface $C = e^*$. Defining $\boldsymbol{H}(\bar{\boldsymbol{\xi}}, e) = \boldsymbol{Q}(\bar{\boldsymbol{\xi}}, e) - \bar{\boldsymbol{\xi}}$ that vanishes at $(\bar{\boldsymbol{\xi}}^*, e^*)$, then the differential with respect to $\bar{\boldsymbol{\xi}}$ is

$$D_{\bar{\boldsymbol{\xi}}}\boldsymbol{H}(\bar{\boldsymbol{\xi}}, e) = D_{\bar{\boldsymbol{\xi}}}\boldsymbol{Q}(\bar{\boldsymbol{\xi}}, e) - D_{\bar{\boldsymbol{\xi}}}\bar{\boldsymbol{\xi}} = M''(\bar{\boldsymbol{\xi}}, e) - Id.$$

Since the eigenvalues of $M''(\bar{\boldsymbol{\xi}}^*, e^*)$ are different from one, $\lambda_3, ..., \lambda_n \neq 1$, then $det(D_{\bar{\boldsymbol{\xi}}}\boldsymbol{H}(\bar{\boldsymbol{\xi}}^*, e^*)) \neq 0$ and the implicit function theorem holds. This means that there exists a neighbourhood I such that $e^* \in I$ and that in this interval $\bar{\boldsymbol{\xi}} = \bar{\boldsymbol{\xi}}(e)$ satisfies $\boldsymbol{Q}(\bar{\boldsymbol{\xi}}(e), e) - \bar{\boldsymbol{\xi}}(e) = \boldsymbol{0}$. □

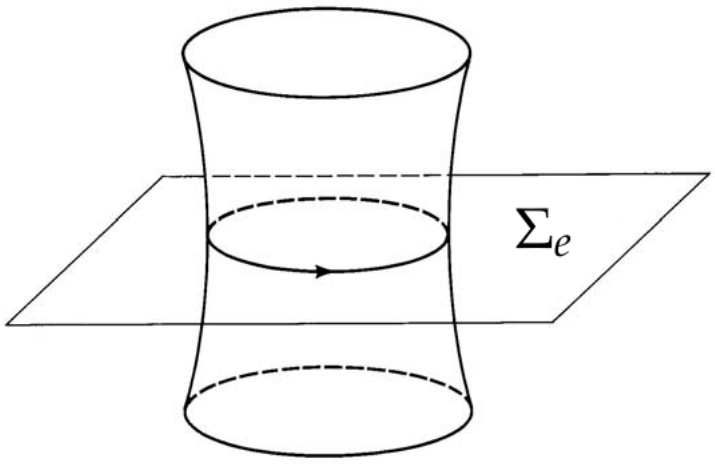

Figure 2.1: Representation of the family of periodic orbits stated by the cylinder theorem. Figure extracted from reference [2].

The cylinder theorem guaranties that if the orbit is an elementary periodic orbit the orbit is grouped in a one-parameter family, as represented in Figure 2.1, as we wanted to prove.

It should be noted that when there is a change of stability along a family of periodic orbits, we cannot apply the implicit function theorem. In this case, the non-linear terms of the flow must be considered to study the possible bifurcations of new families of periodic orbits. This study is not included in the present work.

2.2 Computation of periodic orbits

2.2.1 Numerical continuation of a family of periodic orbits

Now we are in conditions to introduce a method for the continuation of families of periodic orbits, as stated by the cylinder theorem.

Let be

$$\begin{array}{rccc} \boldsymbol{F}: & \mathcal{U} \subseteq \mathbb{R}^{n+1} & \longrightarrow & \mathbb{R}^n \\ & (\bar{\boldsymbol{X}}, x_{n+1}) & \longmapsto & \boldsymbol{F}(\bar{\boldsymbol{X}}, x_{n+1}) \end{array}$$

differentiable (at least once), with $\bar{\boldsymbol{X}} = (x_1, ..., x_n) \in \mathbb{R}^n$. Assume that there are values $\bar{\boldsymbol{X}}^* = (x_1^*, ..., x_n^*)$, x_{n+1}^* such that $\boldsymbol{F}(\bar{\boldsymbol{X}}^*, x_{n+1}^*) = 0$. We will simply denote $\boldsymbol{X} = (\bar{\boldsymbol{X}}, x_{n+1}) = (x_1, ..., x_n, x_{n+1})$. If

$$D\boldsymbol{F} = \begin{pmatrix} \dfrac{\partial F_1}{\partial x_1} & \cdots & \dfrac{\partial F_1}{\partial x_{n+1}} \\ \vdots & \ddots & \\ \dfrac{\partial F_n}{\partial x_1} & & \dfrac{\partial F_n}{\partial x_{n+1}} \end{pmatrix}$$

is the differential of $\boldsymbol{F}$, we denote by $D\boldsymbol{F}_{\boldsymbol{X}\setminus\{x_j\}}$ the squared matrix obtained by not considering the differentiation with respect x_j

$$D\boldsymbol{F}_{\boldsymbol{X}\setminus\{x_j\}} = \begin{pmatrix} \dfrac{\partial F_1}{\partial x_1} & \cdots & \dfrac{\partial F_1}{\partial x_{j-1}} & \dfrac{\partial F_1}{\partial x_{j+1}} & \cdots & \dfrac{\partial F_1}{\partial x_{n+1}} \\ \vdots & \ddots & \vdots & \vdots & \ddots & \vdots \\ \dfrac{\partial F_n}{\partial x_1} & \cdots & \dfrac{\partial F_n}{\partial x_{j-1}} & \dfrac{\partial F_n}{\partial x_{j+1}} & \cdots & \dfrac{\partial F_n}{\partial x_{n+1}} \end{pmatrix},$$

for $j \in \{1, ..., n+1\}$.

Then, if $\det(D\boldsymbol{F}_{\boldsymbol{X}\setminus\{x_j\}}) \neq 0$, by the implicit function theorem, it can be expressed $\boldsymbol{X}\setminus\{x_j\}$ in terms of x_j and if $\boldsymbol{X}\setminus\{x_j\} = \boldsymbol{g}^{(j)}(x_j)$, then

$$\frac{\partial \boldsymbol{g}^{(j)}}{\partial x_j}(x_j) = -D\boldsymbol{F}^{-1}_{\boldsymbol{X}\setminus\{x_j\}}(x_j, \boldsymbol{g}^{(j)}(x_j)) \frac{\partial \boldsymbol{F}}{\partial x_j}(x_j, \boldsymbol{g}^{(j)}(x_j))$$

and each component x_k can be expressed in terms of x_j $j \neq k$.

For $B \in \mathcal{M}_{n\times n}$ satisfying $\det(B) \neq 0$ the expression for its inverse is

$$B^{-1} = \frac{1}{\det(B)} \begin{pmatrix} Ad(B)_{1,1} & \dots & Ad(B)_{n,1} \\ \vdots & \ddots & \\ Ad(B)_{1,n} & & Ad(B)_{n,n} \end{pmatrix},$$

where $Ad(B)_{i,j} = (-1)^{i+j} \det(mB_{i,j})$ is the adjoint and $mB_{i,j}$ is the minor obtained by suppressing the i-th row and j-th column of the matrix B. Denoting $A_j = \det(D\boldsymbol{F}_{\boldsymbol{X}\setminus\{x_j\}})$,

it is possible to compute the determinant of $D\boldsymbol{F}_{\boldsymbol{X}\setminus\{x_k\}}$ using the expansion by minors along the column corresponding to x_j, let's assume that it is j', this results in

$$A_k = \det(D\boldsymbol{F}_{\boldsymbol{X}\setminus\{x_k\}}) = \sum_{i=1}^{n} \frac{\partial F_i}{x_j} Ad(D\boldsymbol{F}_{\boldsymbol{X}\setminus\{x_k\}})_{i,j'} = \sum_{i=1}^{n} \frac{\partial F_i}{x_j}(-1)^{i+j'} \det(mD\boldsymbol{F}_{\boldsymbol{X}\setminus\{x_k\}})_{i,j'} =$$

$$= \sum_{i=1}^{n} \frac{\partial F_i}{x_j}(-1)^{i+j'} \det(mD\boldsymbol{F}_{\boldsymbol{X}\setminus\{x_j\}})_{i,k'} = \sum_{i=1}^{n} \frac{\partial F_i}{x_j}(-1)^{i+j'}(-1)^{i+k'} Ad(D\boldsymbol{F}_{\boldsymbol{X}\setminus\{x_j\}})_{i,k'} =$$

$$= (-1)^{j'+k'} \sum_{i=1}^{n} \frac{\partial F_i}{x_j} Ad(D\boldsymbol{F}_{\boldsymbol{X}\setminus\{x_j\}})_{i,k'} = (-1)^{j+k-1} \sum_{i=1}^{n} \frac{\partial F_i}{x_j} Ad(D\boldsymbol{F}_{\boldsymbol{X}\setminus\{x_j\}})_{i,k'},$$

where k' denotes the column corresponding to x_k when the column corresponding to x_j has been suppressed. The expression for j' and k' is simply $j' = j - I(j > k)$ and $k' = k - I(k > j)$, where $I(\cdot)$ is the indicator function or characteristic function.

It can be seen then that if $x_k^{(j)}$ denotes the component of $\boldsymbol{g}^{(j)}$ referring to the x_k, then

$$\frac{\partial x_k^{(j)}}{\partial x_j} = -\hat{e}_{k'}^T D\boldsymbol{F}^{-1}_{\boldsymbol{X}\setminus\{x_j\}}(x_j, \boldsymbol{g}^{(j)}(x_j)) \frac{\partial \boldsymbol{F}}{\partial x_j}(x_j, \boldsymbol{g}^{(j)}(x_j)) =$$

$$= -\frac{1}{A_j}(Ad(D\boldsymbol{F}_{\boldsymbol{X}\setminus\{x_j\}})_{1,k'}, ..., Ad(D\boldsymbol{F}_{\boldsymbol{X}\setminus\{x_j\}})_{n,k'}) \frac{\partial \boldsymbol{F}}{\partial x_j}(x_j, \boldsymbol{g}^{(j)}(x_j)) =$$

$$= -\frac{1}{A_j} \sum_{i=1}^{n} Ad(D\boldsymbol{F}_{\boldsymbol{X}\setminus\{x_j\}})_{i,k'} \frac{\partial F_i}{\partial x_j}(x_j, \boldsymbol{g}^{(j)}(x_j)) = (-1)^{j+k} \frac{A_k}{A_j}. \tag{2.6}$$

By defining the element of length in $\mathbb{R}^{n+1}$ as $ds^2 = \sum_{k=1}^{n+1} dx_k^2$, and expressing each x_k in terms of x_j, then

$$ds^2 = dx_j^2 + \sum_{\substack{k=1 \\ k\neq j}}^{n+1} d(x_k^{(j)})^2 = dx_j^2 + \sum_{\substack{k=1 \\ k\neq j}}^{n+1} \left(\frac{\partial x_k^{(j)}}{\partial x_j}\right)^2 dx_j^2 = \left(1 + \sum_{\substack{k=1 \\ k\neq j}}^{n+1} \left(\frac{A_k}{A_j}\right)^2\right) dx_j^2,$$

which means that

$$\frac{dx_j}{ds} = \frac{\pm A_j}{\sqrt{\sum_{k=1}^{n+1} A_k^2}}, \tag{2.7}$$

where the sign will depend on the direction along the curve and it must be coherent with Eq. (2.6).

Clearly, this method requires that at least one of the A_j must be different from zero, this means that the rank of $D\boldsymbol{F}$ must be n.

Computation of families of symmetric periodic orbits of the CR3BP

We are interested in periodic orbits of the CR3BP derived from circular Keplerian orbits of the two body problem. These kind of orbits are *simple* [2] and symmetric. This makes their computation easier, since if $P_0 = (x_0, y_0, \dot{x}_0, \dot{y}_0)$ with $y_0 = 0$ and $\dot{x}_0 = 0$, is

[2] Simple in the sense of crossing the x-axis only twice in one period.

the initial condition of one of these orbits, then, in order to fulfil the symmetry condition, it is sufficient to ask that the first intersection with the x-axis of the orbit that passes by P_0, $P_1 = (x_1, y_1, \dot{x}_1, \dot{y}_1)$, satisfies $\dot{x}_1 = 0$ (by definition of P_1, $y_1 = 0$). This is, all points $P_0 = (x_0, 0, 0, \dot{y}_0)$ such that fulfil the following non-linear equation

$$F(P_0) \equiv \dot{x}_1 = 0,$$

are the initial conditions of a symmetric periodic orbit.

To prove this last assertion we need to see that if $(x(t), y(t))$ is a solution, then its mirrored image with respect to the $x = 0$ plane is also a solution, but travelled in opposite direction, i.e $(x(-t), -y(-t))$ is a solution.

As $\Omega = \frac{1}{2}\left((1-\mu)r_1^3 + \mu r_2^3\right) + \frac{1-\mu}{r_1} + \frac{\mu}{r_2}$ only depends on x^2 and y^2, then $\Omega(x, y) = \Omega(x, -y)$. Moreover

$$\Omega_x(x, y) = \left(1 - \frac{1}{r_1^3}\right)(x_1 + \mu)(1 - \mu) + \left(1 - \frac{1}{r_2^3}\right)(x_1 + \mu - 1)\mu = \Omega_x(x, -y)$$

and

$$\Omega_y(x, y) = \left(1 - \frac{1}{r_1^3}\right) y(1 - \mu) + \left(1 - \frac{1}{r_2^3}\right) y\mu = -\Omega_y(x, -y).$$

Therefore, under the change of variables $t'(t) = -t$, $x'(x) = x$ and $y'(y) = -y$, deriving with respect t' we get

$$\frac{dx'}{dt'} = -\dot{x}, \quad \frac{d^2x'}{(dt')^2} = \ddot{x}, \quad \frac{dy'}{dt'} = \dot{y}, \quad \frac{d^2y'}{(dt')^2} = -\ddot{y}.$$

It can be seen that with these new coordinates the differential equations remain invariant

$$\frac{d^2x'}{(dt')^2} - 2\frac{dy'}{dt'} - \Omega_x(x', y') = \ddot{x} - 2\dot{y} - \Omega_x(x, y) = 0,$$

$$\frac{d^2y'}{(dt')^2} + 2\frac{dx'}{dt'} - \Omega_y(x', y') = -\ddot{y} + 2(-\dot{x}) - (-\Omega_y(x, y)) = 0.$$

Since the mirrored image with respect to $y = 0$ is also a solution, the orbits that cross twice the $y = 0$ plane with $\dot{x} = 0$ are symmetric periodic orbits. This is because if $(x(t), y(t))$ is the solution that crosses the x-axis at $t = t_1$ and t_2, then $(x(-t), -y(-t))$ will be a solution in the time interval (t_1, t_2); since the system is autonomous, we can arbitrarily set the initial time, for instance at t_1. Then, we can take $(x(t), y(t))$ as the solution solution in $[0, \tau/2]$ and $(x(-t), -y(-t))$ in $[\tau/2, \tau]$, where $\tau = 2(t_2 - t_1)$. Since both solutions are equal at the boundaries of the interval, the combination of both, let's say $(\varphi(t, \xi))$, is solution in $[0, \tau]$. Moreover, as $\varphi(0, \xi) = \varphi(\tau, \xi)$ it is a periodic solution, as we wanted to see.

As we are working with symmetric periodic orbits in the planar CR3BP, and the sufficient conditions to obtain simple symmetric periodic orbits is that the orbit crosses the x-axis perpendicular to it twice, it is enough to consider the function

$$\begin{array}{rccl} F: & \mathcal{U} \subseteq \mathbb{R}^{1+1} & \longrightarrow & \mathbb{R} \\ & (\xi_x, \xi_{\dot{y}}) & \longmapsto & F(\xi_x, \xi_{\dot{y}}) = \dot{x}(\tau(\xi_x, \xi_{\dot{y}}), \xi_x, 0, 0, \xi_{\dot{y}}), \end{array} \tag{2.8}$$

being $\tau > 0$ the time required to cross the x-axis again for the first time. This means that starting at $(\xi_x, 0, 0, \xi_{\dot{y}})$, i.e, from the x-axis with velocity perpendicular to it, we need to obtain the value of $\dot{x}$ at the first crossing of the x-axis. According to the preceding section, we need to compute the values of A_i

$$A_1 = \frac{\partial F}{\partial \xi_{\dot{y}}} = \frac{\partial \dot{x}}{\partial \tau}\frac{\partial \tau}{\partial \xi_{\dot{y}}} + \frac{\partial \dot{x}}{\partial \xi_{\dot{y}}} \quad \text{and} \quad A_2 = -\frac{\partial F}{\partial \xi_x} = -\left(\frac{\partial \dot{x}}{\partial \tau}\frac{\partial \tau}{\partial \xi_x} + \frac{\partial \dot{x}}{\partial \xi_x}\right),$$

where $\dfrac{\partial \dot{x}}{\partial \xi_x}$ and $\dfrac{\partial \dot{x}}{\partial \xi_{\dot{y}}}$ are the components of A, i.e. $a_{i,j}$, which can be computed by means of the variational equations, as stated in equation (2.3). We also know that $\dfrac{\partial \dot{x}}{\partial \tau}$ is given by the vector-field computed at the final point. It rests to determine $\dfrac{\partial \tau}{\partial \xi_x}$ and $\dfrac{\partial \tau}{\partial \xi_{\dot{y}}}$. For doing so, we will use the restriction that the result lies on the x-axis, and therefore there is a condition h such that

$$h(\xi_x, \xi_{\dot{y}}) = y(\tau(\xi_x, \xi_{\dot{y}}), \xi_x, 0, 0, \xi_{\dot{y}}) = 0,$$

which implies that

$$dh = \frac{\partial y}{\partial \tau}d\tau + \frac{\partial y}{\partial \xi_x}d\xi_x + \frac{\partial y}{\partial \xi_{\dot{y}}}d\xi_{\dot{y}} = 0. \tag{2.9}$$

In addition to that

$$d\tau = \frac{\partial \tau}{\partial \xi_x}d\xi_x + \frac{\partial \tau}{\partial \xi_{\dot{y}}}d\xi_{\dot{y}}. \tag{2.10}$$

Combining Eq. (2.9) and Eq. (2.10) we obtain

$$dh = \left(\frac{\partial y}{\partial \tau}\frac{\partial \tau}{\partial \xi_x} + \frac{\partial y}{\partial \xi_x}\right)d\xi_x + \left(\frac{\partial y}{\partial \tau}\frac{\partial \tau}{\partial \xi_{\dot{y}}} + \frac{\partial y}{\partial \xi_{\dot{y}}}\right)d\xi_{\dot{y}} = 0.$$

As ξ_x and $\xi_{\dot{y}}$ are independent variables, each of the brackets must be zero and, as a result

$$\frac{\partial \tau}{\partial \xi_x} = -\left(\frac{\partial y}{\partial \tau}\right)^{-1}\frac{\partial y}{\partial \xi_x} \quad \text{and} \quad \frac{\partial \tau}{\partial \xi_{\dot{y}}} = -\left(\frac{\partial y}{\partial \tau}\right)^{-1}\frac{\partial y}{\partial \xi_{\dot{y}}}.$$

Finally, putting everything together

$$A_1 = a_{3,4}(\tau, \boldsymbol{\xi}) - \frac{f_{\dot{x}}(\boldsymbol{\varphi}(\tau, \boldsymbol{\xi}))}{f_y(\boldsymbol{\varphi}(\tau, \boldsymbol{\xi}))}a_{2,4}(\tau, \boldsymbol{\xi}) \tag{2.11}$$

and

$$A_2 = -\left(a_{3,1}(\tau, \boldsymbol{\xi}) - \frac{f_{\dot{x}}(\boldsymbol{\varphi}(\tau, \boldsymbol{\xi}))}{f_y(\boldsymbol{\varphi}(\tau, \boldsymbol{\xi}))}a_{2,1}(\tau, \boldsymbol{\xi})\right). \tag{2.12}$$

2.2.2 Refinement

The integration of equations (2.7) requires an initial condition, this means the initial conditions of a periodic orbit; usually, only an approximation of these orbits is known. Furthermore, the continuation procedure is done integrating (2.7) with a low order method,

such as an Adams-Bashforth method. This means that it is mandatory to have a refinement procedure that, given some approximated initial conditions of a periodic orbit, such as the one provided as initial condition or as the result of the integration of equations (2.7), refines them in order to satisfy the periodicity conditions with a certain degree of accuracy. This is done by means of a modified Newton method.

Let be $\boldsymbol{g} : \mathcal{U} \subseteq \mathbb{R}^m \longrightarrow \mathbb{R}^n$ with $m > n$. If we are looking values $\boldsymbol{z} \in \mathcal{U}$ such that $\boldsymbol{g}(\boldsymbol{z}) = 0$ and we have an initial approximation of the value, let's say $\boldsymbol{z}^{(0)}$, we can find an iterative method approximating $\boldsymbol{z}$ more accurate. Linearising around $\boldsymbol{z}^{(k)}$ we obtain

$$\boldsymbol{g}(\boldsymbol{z}^{(k)}) + D\boldsymbol{g}(\boldsymbol{z}^{(k)})\Delta\boldsymbol{z}^{(k)} = \boldsymbol{0}.$$

However, since we have more unknowns than equations we have to impose additional conditions, this conditions can be that the norm of $\Delta\boldsymbol{z}^{(k)}$ is minimal. This norm can be computed in terms of a weight matrix Q as $||\Delta\boldsymbol{z}|| = \Delta\boldsymbol{z}^T Q \Delta\boldsymbol{z}$. This is a problem of conditioned minima, in which we want to minimize the function $F(\Delta\boldsymbol{z}) = ||\Delta\boldsymbol{z}||$ under the constraint $\boldsymbol{G} = \boldsymbol{g}(\boldsymbol{z}) + D\boldsymbol{g}(\boldsymbol{z})\Delta\boldsymbol{z} = \boldsymbol{0}$. This requires the use of Lagrange multipliers.

The Lagrange function will be

$$\mathcal{L}(\Delta\boldsymbol{z}, \Lambda) = \Delta\boldsymbol{z}^T Q \Delta\boldsymbol{z} + \boldsymbol{\Lambda}^T(\boldsymbol{g}(\boldsymbol{z}) + D\boldsymbol{g}(\boldsymbol{z})\Delta\boldsymbol{z}) =$$

$$= \sum_i \sum_j \Delta z_i Q_{i,j} \Delta z_j + \sum_i \Lambda_i g_i(\boldsymbol{z}) + \sum_i \sum_j \Lambda_i (Dg(\boldsymbol{z}))_{i,j} \Delta z_j.$$

Then

$$\frac{\partial \mathcal{L}}{\partial \Delta z_k} = 2\sum_i Q_{k,i}\Delta z_k + \sum_i \Lambda_i (Dg(\boldsymbol{z}))_{i,k}$$

assuming that Q is symmetric and

$$\frac{\partial \mathcal{L}}{\partial \Lambda_k} = g_k(\boldsymbol{z}) + \sum_i (Dg(\boldsymbol{z}))_{k,i}\Delta z_i.$$

Or, in matrix form

$$D_{\Delta\boldsymbol{z}}\mathcal{L} = 2\Delta\boldsymbol{z}^T Q + \boldsymbol{\Lambda}^T D\boldsymbol{g}(\boldsymbol{z}) = \boldsymbol{0} \tag{2.13}$$

and

$$D_{\boldsymbol{\Lambda}}\mathcal{L} = \boldsymbol{g}^T(\boldsymbol{z}) + (D\boldsymbol{g}(\boldsymbol{z})\Delta\boldsymbol{z})^T = \boldsymbol{g}^T(\boldsymbol{z}) + \Delta\boldsymbol{z}^T D\boldsymbol{g}^T(\boldsymbol{z}) = \boldsymbol{0}. \tag{2.14}$$

From (2.13) we get

$$\Delta\boldsymbol{z}^T = -\frac{1}{2}\boldsymbol{\Lambda}^T D\boldsymbol{g}(\boldsymbol{z})Q^{-1}.$$

Replacing Δz^T in (2.14) we can obtain $\boldsymbol{\Lambda}$

$$\boldsymbol{g}^T(\boldsymbol{z}) - \frac{1}{2}\boldsymbol{\Lambda}^T D\boldsymbol{g}(\boldsymbol{z})Q^{-1}D\boldsymbol{g}^T(\boldsymbol{z}) \Rightarrow$$

$$\Rightarrow \boldsymbol{\Lambda}^T = 2\boldsymbol{g}^T(\boldsymbol{z})(D\boldsymbol{g}(\boldsymbol{z})Q^{-1}D\boldsymbol{g}^T(\boldsymbol{z}))^{-1}.$$

Finally, we can write

$$2\Delta\boldsymbol{z}^T Q + 2\boldsymbol{g}^T(\boldsymbol{z})(D\boldsymbol{g}(\boldsymbol{z})Q^{-1}D\boldsymbol{g}^T(\boldsymbol{z}))^{-1}D\boldsymbol{g}(\boldsymbol{z}) = \boldsymbol{0} \Rightarrow$$

$$\Rightarrow \Delta \boldsymbol{z} = -Q^{-1} D\boldsymbol{g}^T(\boldsymbol{z})(D\boldsymbol{g}(\boldsymbol{z})Q^{-1}D\boldsymbol{g}^T(\boldsymbol{z}))^{-1}\boldsymbol{g}(\boldsymbol{z}).$$

This iterative (quadratic) method allows the computation of approximations to the solution of equation $\boldsymbol{g}(\boldsymbol{z}) = \boldsymbol{0}$ with a given accuracy, starting from an approximation. It is well defined whenever the rank of $D\boldsymbol{g}(\boldsymbol{z}^{(k)})$ is n, providing the new approximation as

$$\boldsymbol{z}^{(k+1)} = \boldsymbol{z}^{(k)} - Q^{-1} D\boldsymbol{g}^T(\boldsymbol{z}^{(k)})(D\boldsymbol{g}(\boldsymbol{z}^{(k)})Q^{-1}D\boldsymbol{g}^T(\boldsymbol{z}^{(k)}))^{-1}\boldsymbol{g}(\boldsymbol{z}^{(k)}).$$

Application to the refinement of periodic orbits

According to (2.8), the function we want to obtain a solution ($g \equiv F$), and the norm of $(\Delta\xi_x, \Delta\xi_{\dot{y}})$ to be minimum (with a certain weight matrix Q), we have

$$Dg = \left(\frac{\partial g}{\partial \xi_x} \qquad \frac{\partial g}{\partial \xi_{\dot{y}}}\right) = \left(a_{3,1} - \frac{f_{\dot{x}}}{f_y}a_{2,1} \qquad a_{3,4} - \frac{f_{\dot{x}}}{f_y}a_{2,4}\right),$$

where the components have been computed in the preceding sections.

2.3 Invariant manifolds

2.3.1 Theoretical results

In this section there are introduced briefly some concepts related with the hyperbolic invariant manifolds associated to the periodic orbits. We start with the definition of hyperbolic fixed points.

Definition 2.11. *Let M and N be differentiable manifolds and $\boldsymbol{p} \in M$ a fixed point of the diffeomorphism $\boldsymbol{\psi} : M \longrightarrow N$. It is said that $\boldsymbol{p}$ is a hyperbolic fixed point of $\boldsymbol{\psi}$ if $D\boldsymbol{\psi}(\boldsymbol{p}) : T_{\boldsymbol{p}}M \longrightarrow T_{\boldsymbol{\psi}(\boldsymbol{p})}N$ has no eigenvalue of modulus* 1.

In what follows we will assume that $M = N$. Next we define the global stable and unstable manifolds associated to a hyperbolic fixed point.

Definition 2.12. *Let M be a differentiable manifold and $\boldsymbol{p} \in M$ a hyperbolic fixed point of the diffeomorphism $\boldsymbol{\psi} : M \longrightarrow M$. Then, the stable and unstable manifolds are defined as*

$$\mathcal{W}^s(\boldsymbol{p}) = \{\boldsymbol{q} \in M : \boldsymbol{\psi}^k(\boldsymbol{q}) \to \boldsymbol{p} \quad as \quad k \to +\infty\},$$

$$\mathcal{W}^u(\boldsymbol{p}) = \{\boldsymbol{q} \in M : \boldsymbol{\psi}^{-k}(\boldsymbol{q}) \to \boldsymbol{p} \quad as \quad k \to +\infty\}.$$

In other words, the stable and unstable manifolds are the set of points in M that have $\boldsymbol{p}$ as ω-limit and α-limit, respectively.

Let us see that for a linear diffeomorphism, L, there exist linear subspaces E^s and E^u such that $E^s = \mathcal{W}^s(\boldsymbol{0})$ and $E^u = \mathcal{W}^u(\boldsymbol{0})$. For doing so, it is first presented a proposition that states the decomposition of $\mathbb{R}^n$ in those subspaces.

Proposition 2.13. *If $L \in GL(\mathbb{R}^n)$ is a hyperbolic isomorphism (i.e. it has no eigenvalue of modulus 1) then there exists a unique decomposition $\mathbb{R}^n = E^s \oplus E^u$ such that E^s and E^u are invariant for L and the eigenvalues of $L^s \equiv L|_{E^s}$ and $L^u \equiv L|_{E^u}$ are the eigenvalues of L with modulus less than 1 and larger than 1 respectively.*

Proof. See Palis, J. and de Melo, W. [6] for the proof of a hyperbolic vector field. This proof is completely analogous. □

Now we are in conditions of demonstrate that $E^s = \mathcal{W}^s(\mathbf{0})$ and $E^u = \mathcal{W}^u(\mathbf{0})$ for a linear diffeomorphism.

Proposition 2.14. *If $L \in GL(\mathbb{R}^n)$ is a hyperbolic isomorphism and $\mathbb{R}^n = E^s \oplus E^u$ is the splitting of previous proposition, then $E^s = \mathcal{W}^s(\mathbf{0})$ and $E^u = \mathcal{W}^u(\mathbf{0})$.*

Proof. Let's start seen how is behaved L^k. Considering the Jordan canonical form of L it has been seen in the previous proposition that it can be decomposed in two block matrices J^λ and J^μ for the invariant subspaces E^S and E^u respectively. Each block can be decomposed in J_i^λ and J_j^μ respectively, which are the Jordan canonical blocks of each block. Then $(J^\lambda)^k$ and $(J^\mu)^k$ will be composed by the diagonal blocks $(J_i^\lambda)^k$ and $(J_j^\mu)^k$ respectively. Each block can be represented as $J_i^\gamma = \gamma_i Id + N_1$, where γ stands for λ or μ and N_1 is the matrix defined by elements of the form $(\delta_{r,s-1})$, where $\delta_{i,j}$ is the Kronecker delta function, and Id and N_1 with its correspondent dimension. Moreover, it has been chosen to be $|\lambda_i| < 1$ and $|\mu_j| > 1$. So, if d is the dimension of the J_l^γ block, then, $(N_1)^i = 0$ for $i \geq d$. Hence for $k \geq d$ we will have

$$(J_l^\gamma)^k = \sum_{i=0}^{d} \binom{k}{i} \gamma_l^{k-i} (N_1)^i = \gamma_l^k \sum_{i=0}^{d} \frac{k(k-1)\dots(k-i)}{i!} \gamma_l^{-i} (N_1)^i = \gamma_l^k q_d(k),$$

where $q_d(x)$ is a matrix polynomial of degree at most d. We will have two different behaviours here, $||(J_l^\lambda)^k|| \to 0$ and $||(J_l^\mu)^k|| \to +\infty$ as $\lambda < 1$ and $\mu > 1$.

Now in order to demonstrate that $E^s = \mathcal{W}^s(\mathbf{0})$ there have to be demonstrated that $E^s \subseteq \mathcal{W}^s(\mathbf{0})$ and $\mathcal{W}^s(\mathbf{0}) \subseteq E^s$.

- $E^s \subseteq \mathcal{W}^s(\mathbf{0})$: if $\boldsymbol{v} \in E^s$ then $||L^k \boldsymbol{v}|| = ||(L^s)^k \boldsymbol{v}|| \leq ||(L^s)^k||\, ||\boldsymbol{v}|| \to 0$ as all $||(J_j^\lambda)^k||$ tend to zero, which means that $\boldsymbol{v} \in \mathcal{W}^s(\mathbf{0})$.

- $\mathcal{W}^s(\mathbf{0}) \subseteq E^s$: let's suppose this assumption false, that means that $\exists \boldsymbol{v} \in \mathcal{W}^s(\mathbf{0})$ such that $\boldsymbol{v} \notin E^s$. As $\mathbb{R}^n = E^s \oplus E^u$ then $\boldsymbol{v} = \boldsymbol{u} + \boldsymbol{w}$ such that $\boldsymbol{w} \in E^u$ and therefore $||L^k \boldsymbol{w}|| = ||(L^u)^k \boldsymbol{w}|| \to +\infty$ as all $||(J_j^\mu)^k||$ tend to $+\infty$ and $\mu_j > 1$, which means that $\boldsymbol{v} \notin \mathcal{W}^s(\mathbf{0})$.

The same it is required for $E^u = \mathcal{W}^u(\mathbf{0})$

- $E^u \subseteq \mathcal{W}^u(\mathbf{0})$: if $\boldsymbol{v} \in E^u$ then $||L^{-k} \boldsymbol{v}|| = ||(L^u)^{-k} \boldsymbol{v}|| \leq ||(L^u)^{-k}||\, ||\boldsymbol{v}|| \to 0$ as all $||(J_j^\mu)^{-k}||$ tend to zero ($(J_l^\mu)^{-k} = \gamma_l^{-k} q'_d(k)$) which means that $\boldsymbol{v} \in \mathcal{W}^u(\mathbf{0})$.

- $\mathcal{W}^u(\mathbf{0}) \subseteq E^u$: let's suppose this assumption false, that means that $\exists \boldsymbol{v} \in \mathcal{W}^u(\mathbf{0})$ such that $\boldsymbol{v} \notin E^u$. As $\mathbb{R}^n = E^s \oplus E^u$ then $\boldsymbol{v} = \boldsymbol{u} + \boldsymbol{w}$ such that $\boldsymbol{w} \in E^s$ and therefore $||L^{-k}\boldsymbol{w}|| = ||(L^s)^{-k}\boldsymbol{w}|| \to +\infty$ as all $||(J_j^\lambda)^{-k}||$ tend to $+\infty$ and $\lambda_j^{-1} > 1$, which means that $\boldsymbol{v} \notin \mathcal{W}^u(\mathbf{0})$.

□

Let's now introduce an important theorem, that will not be demonstrated, the Hartman-Grobman theorem.

Theorem 2.15 (Hartman-Grobman theorem)**.** *Let $\boldsymbol{\psi} : M \longrightarrow M$ be a diffeomorphism and let $\boldsymbol{p} \in M$ be a hyperbolic fixed point of $\boldsymbol{\psi}$. Then there exist neighbourhoods $V(\boldsymbol{p}) \subset M$ and $U(\mathbf{0}) \subset T_{\boldsymbol{p}}M$ and a homeomorphism $\boldsymbol{h} : U \longrightarrow V$ such that*

$$\boldsymbol{h} \circ D\boldsymbol{\psi}(\boldsymbol{p}) = \boldsymbol{\psi} \circ \boldsymbol{h}.$$

Proof. See Palis, J. and de Melo, W. [6]. □

The Hartman-Grobman theorem is important because conjugates a diffeomorphism $\boldsymbol{\psi}$ near a hyperbolic fixed point with its differential computed at the fixed point, which is a linear hyperbolic isomorphism.

Let's see some local properties of the stable and unstable manifold. As for each $\boldsymbol{p} \in M$ there $\exists \mathcal{U} \subseteq M$ such that $\mathcal{U}$ is homeomorphic to $\mathbb{R}^n$, let's say by the homeomorphism $H : \mathcal{U} \longrightarrow \mathbb{R}^n$, then let $B_\beta \subseteq H(\mathcal{U})$ the ball of center $H(\boldsymbol{p})$ and radius β in the Euclidean metric of $\mathbb{R}^n$ and let $H^{-1}(B_\beta)$ be the ball in M induced by the homeomorphism then

Definition 2.16. *There are called local stable manifold and local unstable manifold of size β of the point $\boldsymbol{p}$ the sets*

$$\mathcal{W}^s_\beta(\boldsymbol{p}) = \{\boldsymbol{q} \in H^{-1}(B_\beta) : \boldsymbol{\psi}^k(\boldsymbol{q}) \in H^{-1}(B_\beta),\ \ \forall k > 0\},$$

$$\mathcal{W}^u_\beta(\boldsymbol{p}) = \{\boldsymbol{q} \in H^{-1}(B_\beta) : \boldsymbol{\psi}^{-k}(\boldsymbol{q}) \in H^{-1}(B_\beta),\ \ \forall k > 0\}.$$

Proposition 2.17. *If $\beta > 0$ is sufficiently small then:*

(1) $\mathcal{W}^s_\beta(\boldsymbol{p}) \subseteq \mathcal{W}^s(\boldsymbol{p})$ and $\mathcal{W}^u_\beta(\boldsymbol{p}) \subseteq \mathcal{W}^u(\boldsymbol{p})$.

(2) $\mathcal{W}^s_\beta(\boldsymbol{p})$ (resp. $\mathcal{W}^u_\beta(\boldsymbol{p})$) is an embedded topological disc in M whose dimension is that of the stable (unstable) subspace of $L = D\boldsymbol{\psi}(\boldsymbol{p})$.

(3) $\mathcal{W}^s(\boldsymbol{p}) = \bigcup_{k\geq 0} \boldsymbol{\psi}^{-k}(\mathcal{W}^s_\beta(\boldsymbol{p}))$ and $\mathcal{W}^u(\boldsymbol{p}) = \bigcup_{k\geq 0} \boldsymbol{\psi}^k(\mathcal{W}^u_\beta(\boldsymbol{p}))$.

Proof. See Palis, J. and de Melo, W. [6]. □

There is a global result on the stable manifold that, for example, shows that that the stable manifold is tangent to the linear stable manifold of the differential $D\boldsymbol{\psi}(\boldsymbol{p})$.

Theorem 2.18 (The Stable Manifold Theorem)**.** *Let $\boldsymbol{\psi}$ be a diffeomorphism, let $\boldsymbol{p}$ be a hyperbolic fixed point of $\boldsymbol{\psi}$ and E^s the stable subspace of $L = D\boldsymbol{\psi}(\boldsymbol{p})$. Then $\mathcal{W}^s(\boldsymbol{p})$ is a injectively immersed manifold in M and the tangent space to $\mathcal{W}^s(\boldsymbol{p})$ at the point $\boldsymbol{p}$ is E^s.*

Proof. See Palis, J. and de Melo, W. [6]. □

These properties can be translated into the unstable manifold, however, from now on we will be interested in the stable manifold.

2.3.2 Application to periodic orbits

Definition 2.19. *The local stable manifold of the periodic solution $\Gamma = \{\boldsymbol{\varphi}(t, \boldsymbol{\xi}), t \in \mathbb{R}\}$ of 2.2 for a fixed μ is defined as*

$$\mathcal{W}^s_\beta(\Gamma) = \bigcup_{0 \le t < \tau} \mathcal{W}^s(\boldsymbol{\varphi}(t, \boldsymbol{\xi})),$$

where the diffeomorphism considered is $\boldsymbol{Q}_{\boldsymbol{\varphi}(t,\boldsymbol{\xi})}$, the Poincaré in the integral surface of the periodic orbit defined in a neighbourhood of $\boldsymbol{\varphi}(t, \boldsymbol{\xi})$.

In a similar way as in Proposition 2.17, it holds that

Proposition 2.20. *$\mathcal{W}^s(\Gamma) = \bigcup_{t \le 0} \boldsymbol{\varphi}_t(\mathcal{W}^s_\beta(\Gamma))$ where $\boldsymbol{\varphi}_t(\boldsymbol{\xi}) \equiv \boldsymbol{\varphi}(t, \boldsymbol{\xi})$.*

Proof.

- $\bigcup_{t \le 0} \boldsymbol{\varphi}_t(\mathcal{W}^s_\beta(\Gamma)) \subseteq \mathcal{W}^s(\Gamma)$: if $\boldsymbol{\xi} \in \bigcup_{t \le 0} \boldsymbol{\varphi}_t(\mathcal{W}^s_\beta(\Gamma))$ there is a $t' \le 0$ such that $\boldsymbol{\xi} = \boldsymbol{\varphi}_t(\boldsymbol{\xi}')$ where $\boldsymbol{\xi}' \in \mathcal{W}^s_\beta(\Gamma)$, as the application of the Poincaré map to $\boldsymbol{\xi}'$ converges to the fixed point, then $\boldsymbol{\xi}$ will tend to the periodic orbit as $t \to +\infty$.
- $\mathcal{W}^s(\Gamma) \subseteq \bigcup_{t \le 0} \boldsymbol{\varphi}_t(\mathcal{W}^s_\beta(\Gamma))$: if $\boldsymbol{\xi} \in \mathcal{W}^s(\Gamma)$ there exists a t' such that $\boldsymbol{\varphi}(t, \boldsymbol{\xi})$ intersects Σ at $\boldsymbol{\varphi}(t', \boldsymbol{\xi})$ and then the application of the Poincaré map is convergent to the fixed point, that means that $\boldsymbol{\varphi}(t', \boldsymbol{\xi}) \in \mathcal{W}^s_\beta(\Gamma)$ or in other words that $\boldsymbol{\xi} \in \boldsymbol{\varphi}_{-t'}(\mathcal{W}^s_\beta(\Gamma)) \subseteq \bigcup_{t \le 0} \boldsymbol{\varphi}_t(\mathcal{W}^s_\beta(\Gamma))$

□

Then, according to the Stable Manifold Theorem (2.18), the tangent space to $\mathcal{W}^s(\Gamma)$ at the point $\boldsymbol{\varphi}(t, \boldsymbol{\xi})$ is direct sum of the linear subspace created by the direction of the flow and the stable subspace of $D\boldsymbol{Q}_{\boldsymbol{\varphi}(t,\boldsymbol{\xi})}$, say E^s, at the equilibrium point, or in other words the stable subspace of M'' the associated monodromy matrix of the Poincaré map in the integral surface. We will be, however, interested in E^s, which is the direction of the stable manifold for the Poincaré map in the integral surface.

Let us see that the eigenvalues do not change along the periodic orbit and, therefore, the stable manifold of the orbit is well defined.

Proposition 2.21. *Let be $\boldsymbol{\varphi}(t,\boldsymbol{\xi})$ a periodic solution of period τ and let $M(\boldsymbol{\xi})$ be the monodromy matrix of the periodic solution computed at $\boldsymbol{\xi}$, then $M(\boldsymbol{\varphi}(t,\boldsymbol{\xi})) = A(t,\boldsymbol{\xi})M(\boldsymbol{\xi})A^{-1}(t,\boldsymbol{\xi})$, where $A(t,\boldsymbol{\xi})$ is the solution of Eq. 2.3.*

Proof. Let's first demonstrate that

$$A(t+t',\boldsymbol{\xi}) = A(t,\boldsymbol{\varphi}(t',\boldsymbol{\xi}))A(t',\boldsymbol{\xi}). \tag{2.15}$$

Consider $B(t) = A(t,\boldsymbol{\varphi}(t',\boldsymbol{\xi}))A(t',\boldsymbol{\xi})$ and let's see that both sides of the equality satisfy the same initial value problem. For the left side of the equation we have

$$\begin{cases} \dot{A}(t+t',\boldsymbol{\xi}) = D\boldsymbol{f}(\boldsymbol{\varphi}(t+t',\boldsymbol{\xi}))A(t+t',\boldsymbol{\xi}), \\ A(0+t',\boldsymbol{\xi}) = A(t',\boldsymbol{\xi}), \end{cases} \tag{2.16}$$

and as

$$\dot{B}(t) = \dot{A}(t,\boldsymbol{\varphi}(t',\boldsymbol{\xi}))A(t',\boldsymbol{\xi}) = D\boldsymbol{f}(\overbrace{\boldsymbol{\varphi}(t,\boldsymbol{\varphi}(t',\boldsymbol{\xi}))}^{\boldsymbol{\varphi}(t+t',\boldsymbol{\xi})})\overbrace{A(t,\boldsymbol{\varphi}(t',\boldsymbol{\xi}))A(t',\boldsymbol{\xi})}^{B},$$

then

$$\begin{cases} \dot{B}(t) = D\boldsymbol{f}(\boldsymbol{\varphi}(t+t',\boldsymbol{\xi}))B(t), \\ B(0) = A(0,\boldsymbol{\varphi}(t',\boldsymbol{\xi}))A(t',\boldsymbol{\xi}) = IdA(t',\boldsymbol{\xi}) = A(t',\boldsymbol{\xi}). \end{cases} \tag{2.17}$$

As both initial value problems are the same, we can conclude that Eq. (2.15) is true.

Consider now

$$A(t+\tau,\boldsymbol{\xi}) = A(t,\boldsymbol{\varphi}(\tau,\boldsymbol{\xi}))A(\tau,\boldsymbol{\xi}) = A(t,\boldsymbol{\xi})M(\boldsymbol{\xi}) \tag{2.18}$$

and

$$A(\tau+t',\boldsymbol{\xi}) = M(\boldsymbol{\varphi}(t',\boldsymbol{\xi}))A(t',\boldsymbol{\xi}), \tag{2.19}$$

then, for $t = \tilde{t}$ in (2.18) and $t' = \tilde{t}$ in (2.19) both equations must be equal, so

$$A(\tilde{t},\boldsymbol{\xi})M(\boldsymbol{\xi}) = M(\boldsymbol{\varphi}(\tilde{t},\boldsymbol{\xi}))A(\tilde{t},\boldsymbol{\xi}),$$

and, therefore

$$M(\boldsymbol{\varphi}(\tilde{t},\boldsymbol{\xi})) = A(\tilde{t},\boldsymbol{\xi})M(\boldsymbol{\xi})A^{-1}(\tilde{t},\boldsymbol{\xi}),$$

as we wanted to prove. □

Proposition 2.22. *The eigenvalues of the monodromy matrix do not change along the periodic orbit.*

Proof. Let $M(\boldsymbol{\varphi}(t,\boldsymbol{\xi}))$ be the monodromy matrix along the periodic orbit. Let us see that its eigenvalues do not change. From proposition 2.21 we have that

$$M(\boldsymbol{\varphi}(t,\boldsymbol{\xi}))A(t,\boldsymbol{\xi}) = A(t,\boldsymbol{\xi})M(\boldsymbol{\xi}),$$

then, if $\boldsymbol{u}_0$ is a eigenvector of the monodromy matrix $M(\boldsymbol{\xi})$ of eigenvalue λ

$$M(\boldsymbol{\varphi}(t,\boldsymbol{\xi}))A(t,\boldsymbol{\xi})\boldsymbol{u}_0 = A(t,\boldsymbol{\xi})M(\boldsymbol{\xi})\boldsymbol{u}_0 = \lambda A(t,\boldsymbol{\xi})\boldsymbol{u}_0,$$

being, therefore, $\boldsymbol{u}_t \equiv A(t,\boldsymbol{\xi})\boldsymbol{u}_0$ an eigenvector of the monodromy matrix $M(\boldsymbol{\varphi}(t,\boldsymbol{\xi}))$ with eigenvalue λ. □

This previous proposition guaranties the definition of the stability of a periodic orbit and provides a method for obtaining the eigenvectors of the monodromy matrix along the orbit in terms of an initial one.

Chapter 3

Implementation and numerical results

In this chapter we explain how the methods exposed in the previous one have been applied and implemented, as well as some of the methods that have been used for the integration of differential equations, and for the computation of eigenvectors and eigenvalues. We also present the results obtained for the periodic orbits around Mars, as well as their associated stable manifolds.

The main references used for this chapter are [8], [10], [11] and [12].

3.1 Computation of periodic orbits

The integration of the differential equations driving the dynamical system (CR3BP equations) has been done using a Runge-Kutta-Fehlberg method. This method belongs to the family of Runge-Kutta methods that allow an adaptive integration step. The method used in this work is the RKF78, which is of order seven and with an error estimator of order eight. This method computes the solution using the RK7, and the RK8 estimates the error, allowing in this way to adapt the time step, optimising the computational time and providing a control of the local truncation error.

The integration of the differential equations (2.7) of the continuation procedure has been done using a linear multi-step method. When the equations (2.7) are applied to (2.8), i.e. using coefficients (2.11) and (2.12) we get

$$\frac{dx}{ds} = \frac{a_{3,4} - \frac{f_{\dot{x}}}{f_y} a_{2,4}}{\sqrt{\left(a_{3,1} - \frac{f_{\dot{x}}}{f_y} a_{2,1}\right)^2 + \left(a_{3,4} - \frac{f_{\dot{x}}}{f_y} a_{2,4}\right)^2}},$$

$$\frac{d\dot{y}}{ds} = -\frac{a_{3,1} - \frac{f_{\dot{x}}}{f_y}a_{2,1}}{\sqrt{\left(a_{3,1} - \frac{f_{\dot{x}}}{f_y}a_{2,1}\right)^2 + \left(a_{3,4} - \frac{f_{\dot{x}}}{f_y}a_{2,4}\right)^2}},$$

where $a_{i,j}$ are the components of the matrix $A(\tau)$ obtained integrating the variational equations (2.3) until reach the first intersection.

The multi-step method used has been the so-called Adams-Bashforth of fix step or explicit multi-step of fix step, reference [12].

3.1.1 The Adams-Bashforth multi-step method

Let be

$$\begin{array}{rccc} \boldsymbol{f}: & \mathcal{U} \subseteq \mathbb{R}^n & \longrightarrow & \mathbb{R}^m \\ & \boldsymbol{x} & \longmapsto & \boldsymbol{f}(\boldsymbol{x}) \end{array} \tag{3.1}$$

defining the differential equation $\dot{\boldsymbol{x}} = \boldsymbol{f}(\boldsymbol{x})$ to be solved.

The multi-step methods are characterized by interpolating the function $\boldsymbol{f}$ by a polynomial of degree $r-1$ by means of r evaluations in different points of $\boldsymbol{f}$. Integrating the polynomial along one step it is obtained the solution at the next time by means of the fundamental theorem of calculus

$$\boldsymbol{x}_{k+r} - \boldsymbol{x}_{k+r-1} = \int_{t_{k+r-1}}^{t_{k+r}} \boldsymbol{f}(\boldsymbol{x})dt.$$

This method is of order r due to the fact that it has been integrated a polynomial of order $r-1$ and therefore the error that was of order r will be of order $r+1$. The approximated solution will be

$$\hat{\boldsymbol{x}}_{k+r} = \hat{\boldsymbol{x}}_{k+r-1} + h\sum_{i=0}^{r-1} \beta_{k+i}\boldsymbol{f}_{k+i}\ ,$$

where h is the step, $\boldsymbol{f}_j$ the evaluation of the function $\boldsymbol{f}$ at the node $\boldsymbol{x}_j$ and β_j are coefficients found in tables, resulting from the integration of the interpolation polynomial.

This method is useful in our case combined with the method of refinement of the orbit. By means of this method it is possible to obtain an approximation to the "next" orbit separated by a step Δs obtaining values x and $\dot{y}$ that will be refined to obtain values x_{ref} and $\dot{y}_{ref}$ that will be used to compute the values $a_{i,j}$ and used to compute the continuation again.

The order of the multi-step used in the computations has been of order four, however, when the first orbit is derived as we only have this one to be used, it has to be used a multi-step of order one, which is equivalent to the Euler method. Then after obtaining the second periodic orbit and being refined this one, we have two orbits to be used and then it is possible to make use of a multi-step of order two, and so on until we have four orbits and then we keep the integrator at order four, discarding the "older" orbit being used.

3.1.2 The modified Newton method

Although in the previous chapter we have mentioned the possibility of using any weight matrix Q to compute the norm of the correction in the modified Newton method,

in this work we have taken Q as the identity, resulting in the same weight for the position x and the velocity $\dot{y}$. This produces the following formula for the refinement, according to what has been explained in the previous chapter

$$\begin{pmatrix} \xi_x^{(k+1)} \\ \xi_{\dot{y}}^{(k+1)} \end{pmatrix} = \begin{pmatrix} \xi_x^{(k)} \\ \xi_{\dot{y}}^{(k)} \end{pmatrix} - \begin{pmatrix} a_{3,1} - \frac{f_{\dot{x}}}{f_y} a_{2,1} \\ \\ a_{3,4} - \frac{f_{\dot{x}}}{f_y} a_{2,4} \end{pmatrix} \left(\left(a_{3,1} - \frac{f_{\dot{x}}}{f_y} a_{2,1} \right)^2 + \left(a_{3,4} - \frac{f_{\dot{x}}}{f_y} a_{2,4} \right)^2 \right)^{-1} \dot{x},$$

where the vector-field $\boldsymbol{f}$, the coefficients of the A matrix, and $\dot{x}$ are evaluated at the first intersection of the orbit with the x-axis.

3.1.3 Numerical results

The periodic solutions of the two body problem have been continued in the CR3BP. In order to find the initial conditions of the orbits that will generate the family of periodic orbits of the CR3BP, we have used the initial conditions of the two body problem orbits. In an inertial Cartesian coordinate system, the circular orbits of Kepler's problem can be determined equating the centripetal force with the gravitational force due to the primary

$$\frac{(v^c)^2}{r_2^c} = \frac{Gm_2}{(r_2^c)^2},$$

where v^c is the modulus of the velocity and r_2^c is the distance between the small mass and the satellite. Then, in dimensionless coordinates we have the relation $v = \sqrt{\frac{\mu}{r_2}}$, which is the velocity of rotation around the primary and the parameter $\mu = 3.2270 \cdot 10^{-7}$. However, as the reference system is a rotating frame, there is a intrinsic rotation with respect to the primary as shown in Figure 3.1. In order to compensate this effect of the rotation, we take the difference between the velocity due to the rotation of the primary and the satellite around the center of mass. That is $\Delta v^{rot} = v_3^{rot} - v_2^{rot} = (1 - \mu + r_2) \cdot 1 - (1 - \mu) \cdot 1 = r_2$ compensates the intrinsic rotation.

Direct orbits

Direct orbits are orbits with the same direction of rotation as the non-inertial (synodic) system, that is: counterclockwise. Therefore, the approximated initial conditions for these direct orbits will be

$$(x, y, \dot{x}, \dot{y}) = \left(1 - \mu - r_2, 0, 0, -\sqrt{\frac{\mu}{r_2}} + r_2 \right), \tag{3.2}$$

where the initial position has been taken at the left of the small mass and, as a consequence, the velocity must be negative in order rotate counterclockwise. Note that the correction due to the non-inertial system is making the velocity smaller in modulus, this is because there is already a contribution in the direction of rotation.

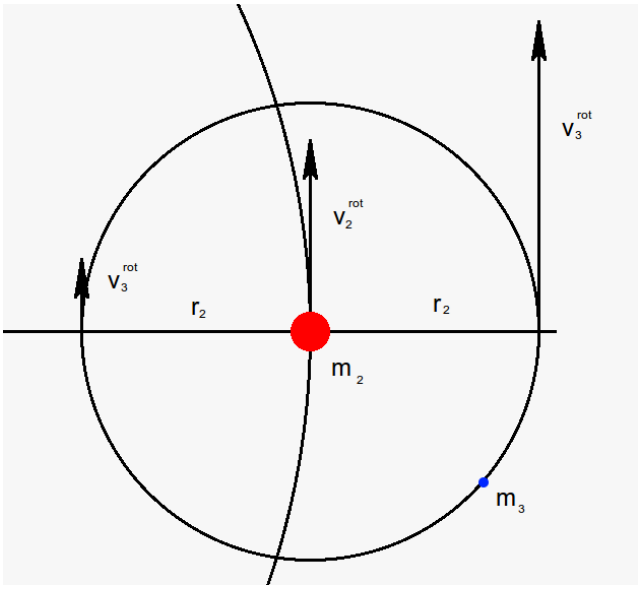

Figure 3.1: Image representing the intrinsic rotation in the rotating frame. When the velocity in the rotating system is zero, there is still some velocity in the direction of the rotation of the system, which increases linearly with the distance to the center of mass according to $v = r\dot{\theta}$, and this creates the effect of rotation in the direct direction.

Figure 3.2 shows a discrete set of orbits of the family of direct orbits around the small primary that have been computed. One can see that the first orbits of the family are almost circular orbits around the small primary. When the family is continued, the orbits start to be more eccentric and get closer to the small primary from the right side even though they go further from the left side. The family ends when a collision orbit with Mars is reached (although the family can be continued further, regularizing the differential equations of the CR3BP, this has not been done this work). It is observed that this family of orbits remains really close to the primary, being the furthest point of the orbit at about $4 \cdot 10^{-3}$ from the primary.

Retrograde orbits

The retrograde orbits are the orbits with the direction of rotation opposite to the one of the synodic system, that is to say clockwise. Then, the approximated initial conditions for these retrograde orbits will be

$$(x, y, \dot{x}, \dot{y}) = \left(1 - \mu + r_2, 0, 0, -\sqrt{\frac{\mu}{r_2}} - r_2\right). \tag{3.3}$$

The initial position has been taken at the right side of the small mass and, as a consequence, the velocity must be negative in order rotate clockwise. Note that the correction due to the non-inertial system is making the velocity larger in modulus and this is because there is a contribution in the direction of rotation that has to be compensated.

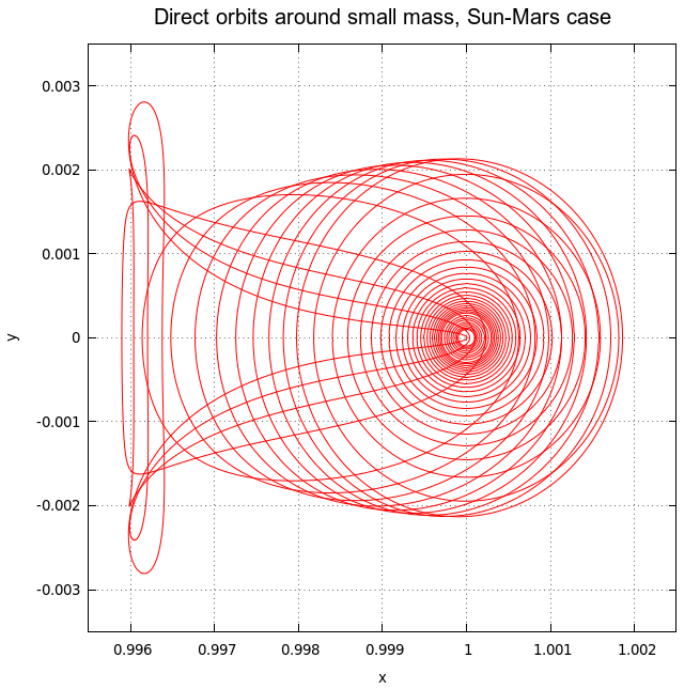

Figure 3.2: Family of direct orbits around Mars in rotating dimensionless coordinates. The starting orbit is the refined orbit that has the initial conditions $\xi_x = 0.9999$ and $\xi_{\dot{y}} = -0.0567988925$ from the Kepler approximation, that means a distance of $r_2 \approx 10^{-4}$ from the satellite to Mars.

The reason why the initial conditions are at the left side of the primary for the direct orbits, and in the right side for the retrograde ones, will be justified later when we give the results of their stability parameters.

In the Figure 3.3 is harder to see that the orbits start being almost circular orbits around the primary because of the range of the plot, however they start being nearly circular orbits as happens with the direct orbits. This orbits are more elongated in the y-axis and grow in size until they reach a collision orbit with the Sun (although this family can also be continued further than the collision orbit). These orbits increase in period as they increase in size up to more than 6 units of time, or approximately one Martian year ($\sim$ 700 days).

3.2 Computation of manifolds

In this section we define the stability parameter of a periodic orbit; according to the value of this parameter we classify the orbits and determine if they have a stable manifold associated. We also explain how the power method for the computation the eigenvectors and eigenvalues of greatest modulus is used, and finally we present the numerical results obtained.

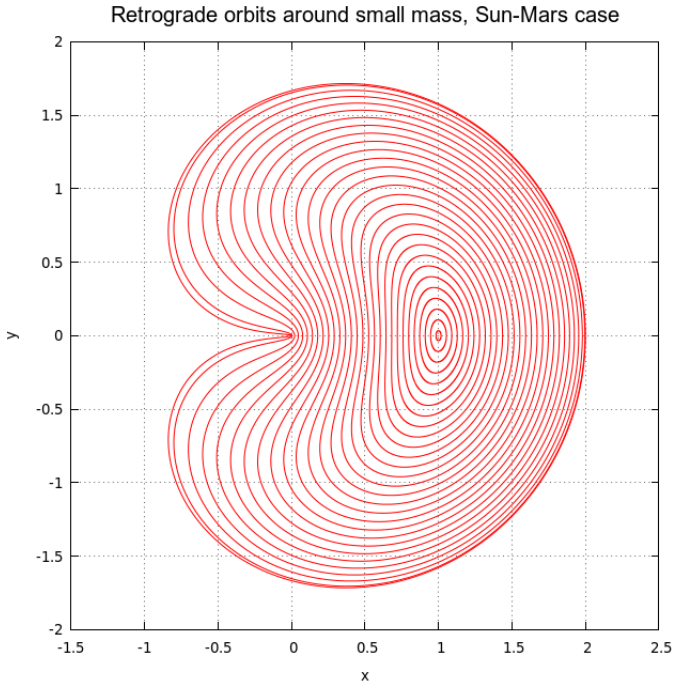

Figure 3.3: Family of retrograde orbits around Mars in rotating dimensionless coordinates. The starting orbit is the refined orbit that has the initial conditions $\xi_x = 1.0000993546$ and $\xi_{\dot{y}} = -0.0569982471$ from the Kepler approximation, that means a distance of $r_2 \approx 10^{-4}$ from the satellite to Mars.

3.2.1 The stability parameter

As it has been seen in the previous chapter, the eigenvalues of the monodromy matrix remain constant along the whole periodic orbit, therefore it has sense to speak about the stability of the orbit. As it has already been said, the monodromy matrix has at least two eigenvalues of value $+1$ corresponding to the direction tangent to the orbit and the direction of the gradient of the Jacobi constant . The remaining eigenvalues correspond to the eigenvalues of the Poincaré map in the integral surface. As this map is a discrete one, the eigenvalues with modulus greater than one define the unstable direction, the eigenvalues with modulus smaller than one the stable direction and the ones with the modulus exactly one define the center direction. Since our system is Hamiltonian, according to Liouville's theorem, the determinant of the monodromy matrix must be $+1$ and therefore $\det(M) = \prod_{i=1}^{4} \lambda_i = 1 \cdot 1 \cdot \lambda_1 \cdot \lambda_2 = +1$. As a consequence: $\lambda = \lambda_1 = \lambda_2^{-1}$. This allows the following definition:

Definition 3.1. *The stability parameter of a periodic orbit of the CR3BP is defined as as*

$$Tr = \lambda + \lambda^{-1}.$$

Since our monodromy matrix is a real valued matrix, the stability parameter is real

$Tr = trace(M) - 2 \in \mathbb{R}$. This means that $\lambda^* = \lambda^{-1}$ and as a result: either $\lambda \in \mathbb{R}$, or $\lambda \in \mathbb{C}$ and $|\lambda| = 1$. From this relation between the eigenvalues whenever there is a eigenvalue of modulus greater than one the other will be smaller than one, making the fixed point associated to the Poincaré map an hyperbolic fixed point in the integral surface and therefore with a stable direction and an unstable direction associated. That results in an unstable orbit. The stability parameter helps us in this classification, because if the eigenvalues are of modulus one we will have that $|Tr| \leq 2$ and $|Tr| > 2$ otherwise.

Then if the periodic orbit is unstable, i.e. $|Tr| > 2$, that means that one of the eigenvalues is larger than the other and larger in modulus than one, therefore it can be used the power method in order to obtain in an easy straightforward way the eigenvalue and eigenvector.

3.2.2 Power method

The power method, or power iteration, is an iterative algorithm for for the computation of the dominant eigenvector of a matrix. The algorithm works as follows: given a matrix A and a nonzero initial vector v_0, the iterate $A^k v_0$ converges to the dominant eigenvector under reasonably mild conditions. The dominant eigenvector is defined as the eigenvector associated with the eigenvalue of largest modulus.

In order to avoid numerical overflow it is convenient to normalize the vector after each iteration. A possible choice for the normalization is to take α_k as the largest component of the vector v_k and then consider the normalized vector as $\hat{v}_k = \dfrac{v_k}{\alpha_k}$.

The following theorem establishes a convergence result for described procedure.

Theorem 3.2. *Assume that there is one and only one eigenvalue λ_1 of A of largest modulus, i.e λ_1 has algebraic and geometric multiplicity one. Then either the initial vector v_0 has no component in the invariant subspace associated with λ_1 or the sequence of vectors generated by the algorithm converges to an eigenvector associated with λ_1 and α_k converges to λ_1.*

Proof. We have that the k normalized iterate is $\hat{v}_k = \prod_{i=0}^{k} \dfrac{1}{\alpha_i} A^k \hat{v}_0$. Consider $A = PJP^{-1}$ where J is the Jordan canonical form and P is the matrix of change of basis, then J is composed by block matrices $J_l = \lambda_l Id + N_1$, where N_1 is the matrix defined by elements of the form $(\delta_{r,s-1})$, being $\delta_{i,j}$ the Kronecker delta that is one when the subindex are equal and zero otherwise. Then as $A^k = PJ^kP^{-1}$, let's see what happens with J^k.

As J is a diagonal block matrix, then J^k will be composed by the diagonal blocks J_l^k. Then $J_l^k = \sum_{i=0}^{k} \binom{k}{i} \lambda_l^{k-i} Id N_1^i = \sum_{i=0}^{k} \binom{k}{i} \lambda_l^{k-i} N_i$, where $N_1^i = N_i = (\delta_{r,s-i})$. If d is the dimension of the J_l block, then $N_i = 0$ for $i \geq d$. Then for $k \geq d$ we will have

$$J_l^k = \sum_{i=0}^{d} \binom{k}{i} \lambda_l^{k-i} N_i = \sum_{i=0}^{d} \frac{k!}{i!(k-i)!} \lambda_l^{k-i} N_i = \sum_{i=0}^{d} \frac{k(k-1)\dots(k-i)}{i!} \lambda_l^{k-i} N_i = \sum_{i=0}^{d} p_i(k) \lambda_l^{k-i} N_i,$$

where $p_i(x)$ is a polynomial of degree at most i. If now is considered $\dfrac{1}{\lambda_1} J_l$ then

$$\left(\frac{1}{\lambda_1} J_l\right)^k = \frac{1}{\lambda_1^k} \sum_{i=0}^{d} p_i(k) \lambda_l^{k-i} N_i = \sum_{i=0}^{d} p_i(k) \frac{\lambda_l^{k-i}}{\lambda_1^k} N_i = \sum_{i=0}^{d} p_i(k) \left(\frac{\lambda_l}{\lambda_1}\right)^k \lambda_l^{-i} N_i =$$

$$= \left(\frac{\lambda_l}{\lambda_1}\right)^k \sum_{i=0}^{d} p_i(k)\lambda_l^{-i} N_i = \left(\frac{\lambda_l}{\lambda_1}\right)^k q_d(k),$$

where q_d is a matrix polynomial of degree at most d. Therefore this expression, as $\lambda_1 > \lambda_l$ for all $l \neq 1$, tend to zero as k tend to infinity. This means that $\left(\frac{1}{\lambda_1} J\right)^k$ tend to a matrix where only the element of the first row and first column is 1 (because λ_1 has algebraic and geometric multiplicity one) and the rest is zero. Since the element of the first row and first column is 1 for each k we will have that

$$\hat{v}_k = \prod_{i=0}^{k} \frac{1}{\alpha_i} A^k \hat{v}_0 = \left(\lambda_1^k \prod_{i=0}^{k} \frac{1}{\alpha_i}\right) P \left(\frac{1}{\lambda_1} J\right)^k P^{-1} \left(\sum_{i=1}^{n} u_{i_0}\right) =$$

$$= \left(\lambda_1^k \prod_{i=0}^{k} \frac{1}{\alpha_i}\right) \left(u_{1_0} + P \left(\frac{1}{\lambda_1} J\right)^k P^{-1} \left(\sum_{i=2}^{n} u_{i_0}\right)\right),$$

where $\hat{v_0} = \sum_{i=1}^{n} u_{i_0}$ is the decomposition of $\hat{v_0}$ in terms of the vectors of the canonical base. Then the right term of the multiplication converges to u_{1_0} and it only has to be seen that α_k converges to λ_1, but this is a consequence of $A\hat{v}_{k-1} = \alpha_k \hat{v}_k$ and the convergence of v_k to the eigenvector of eigenvalue λ_1.

If $u_{1_0} = 0$, i.e. the initial vector v_0 has no component in the invariant subspace associated with λ_1, it will not converge to the desired value. □

The above algorithm is only valid to find the eigenvector associated with the eigenvalue of largest modulus, but it can be used to find the one of the smallest modulus by applying the method to its inverse.

3.2.3 Numerical results

In this section we present the numerical results obtained for the stability parameters of the two families of periodic orbits computed, together with the ones of the stable manifolds associated to them.

Stability parameter

The reason why the initial approximation of the direct orbits is at the left side of the mass and for the retrograde orbits is in the right side is because of the computation of the stability parameter. As the stability parameter is computed after one revolution, if the orbit is started near one of the primaries after one revolution the computation of the monodromy matrix ends near the primary and therefore small discrepancies in the time of arrival could create big errors in the stability parameter. When the parameter has been computed in this way it has been observed a noisy output, being more practical avoid this situation. As in the two cases the family propagation makes the orbit approach the collision orbit it has been chosen the starting point that is further from the mass. In the case of the direct orbits the orbits begin to get closer by the right of the small mass and therefore it is more convenient to compute the orbits starting from the left side. For the

retrograde orbits it happens that the orbits approach the greater mass and therefore it is more convenient to compute the orbits starting from the right of the small mass.

After the computation of the stability parameter along the family of retrograde orbits it can be seen that these orbits are stable, since the stability parameter is bounded between $+2$ and -2 being around $+2$ the most of the time. This mean that the family of retrograde orbits is not of our interest because no stable manifold exists.

It has to be said that both families here found can be continued further than the collision orbit, resulting in more complex orbits. These orbits are unstable and also stop being simple and they start to cross the x-axis more than twice per period. Although they might be of our interest, the further exploration of these families of orbits is beyond the scope of this work.

In both figures 3.4 and 3.5 are represented the stability parameter, in green, and the Jacobi constant, in red, versus the initial condition in position ξ_x. As for the initial conditions $\xi_y = 0$ and $\xi_{\dot{x}} = 0$, then the Jacobi constant give us idea of $\xi_{\dot{y}}$ by the relation Eq. (1.23).

Stable manifold

The stable manifold in our case is a two dimensional manifold and will be computed by means of a linear approximation. There have been selected several unstable orbits in order to compute its stable manifold. For the computation of this manifolds it has been divided the period of the orbit by n resulting in n points over the orbit.

Then for each of the selected points there has been computed the eigenvectors along the orbit that will define the stable direction of orbit and therefore its linear approximation to the manifold. In order to compute these eigenvectors it has been computed the monodromy matrix at the initial condition $M((\xi_x, 0, 0, \xi_{\dot{y}})^T)$ and then using the power method explained in section 3.2.2 it has been computed the eigenvalue of smallest modulus, i.e. the one in the direction of the stable manifold. Once the eigenvector has been found at the initial conditions, $\boldsymbol{u}_0$, it has been transported along the n points over the orbit using the method derived from proposition 2.22, i.e. $\boldsymbol{u}_{t_j} = A\left(\frac{j}{n}\tau, \boldsymbol{\xi}\right)\boldsymbol{u}_0$ with $j \in \{0, ..., \tau - 1\}$ and being normalized.

Then for each of the selected points it has been added a perturbation along the stable direction, in both directions, positive and negative: $\boldsymbol{\varphi}\left(\frac{j}{n}\tau, \boldsymbol{\xi}\right) \pm \epsilon \boldsymbol{u}_{t_j}$. This perturbed state has been integrated backward in order to find the approximation to the stable manifold. For the computations it has been chosen $n = 100$. Examples of this manifold are Figures 3.6, 3.7 and 3.8a.

Once the stable manifold for each orbit has been computed, the distance of this manifold to the Earth can be computed, which it has been our objective. In order to compute this distance, it has been computed the distance to the origin and it has been subtracted the mean Sun-Earth distance. Although this measure of the distance to the stable manifold to the Earth is an approximation it is sufficiently good enough due to the small μ of both Earth and Mars. The mean Sun-Earth distance has been chosen to be $d_{S-E} \approx 0.656313$ in the dimensionless coordinate system of the Sun-Mars problem. This means that the

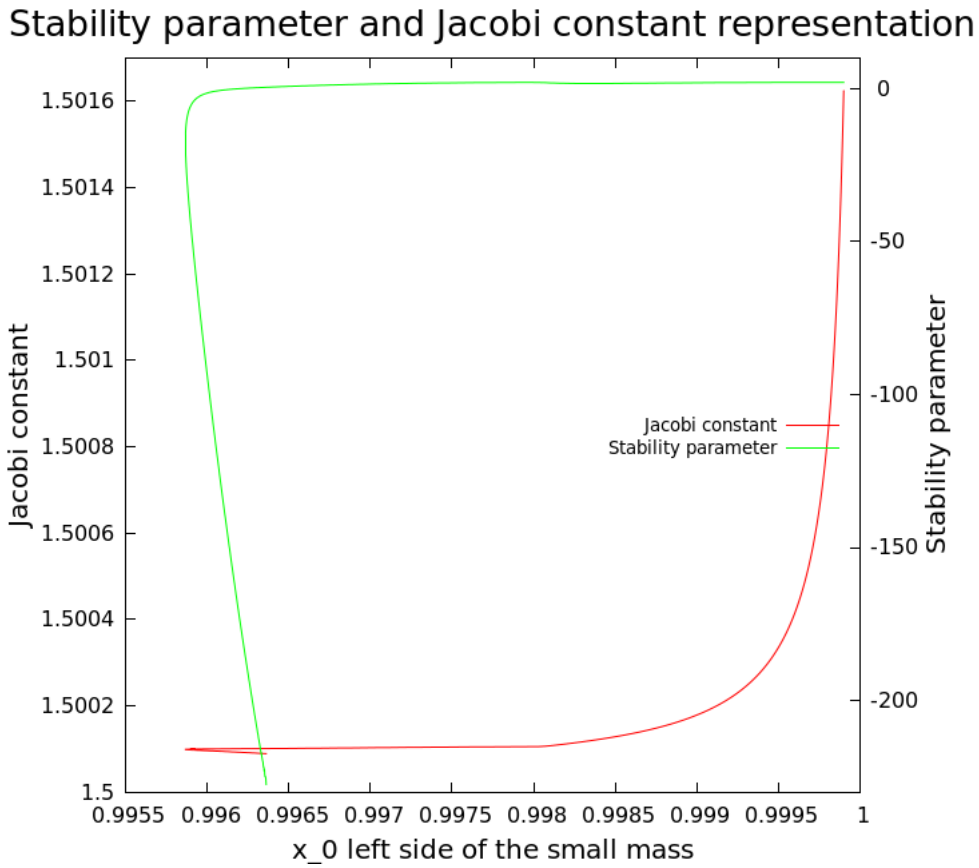

Figure 3.4: In this figure can be observed that the direct orbits become unstable approximately when the initial condition in position reach the maximum distance from the primary, i.e. when the loops observed in Figure 3.2 start to form. In order to read properly this figure it has to be read from right to left, because the orbits start from nearly $\xi_x \approx 1$. We remark that the Jacobi constant is almost the same along the whole family. This can make easy the transfer between orbits of the family. The starting orbit in this generation has been the same as in Figure 3.2.

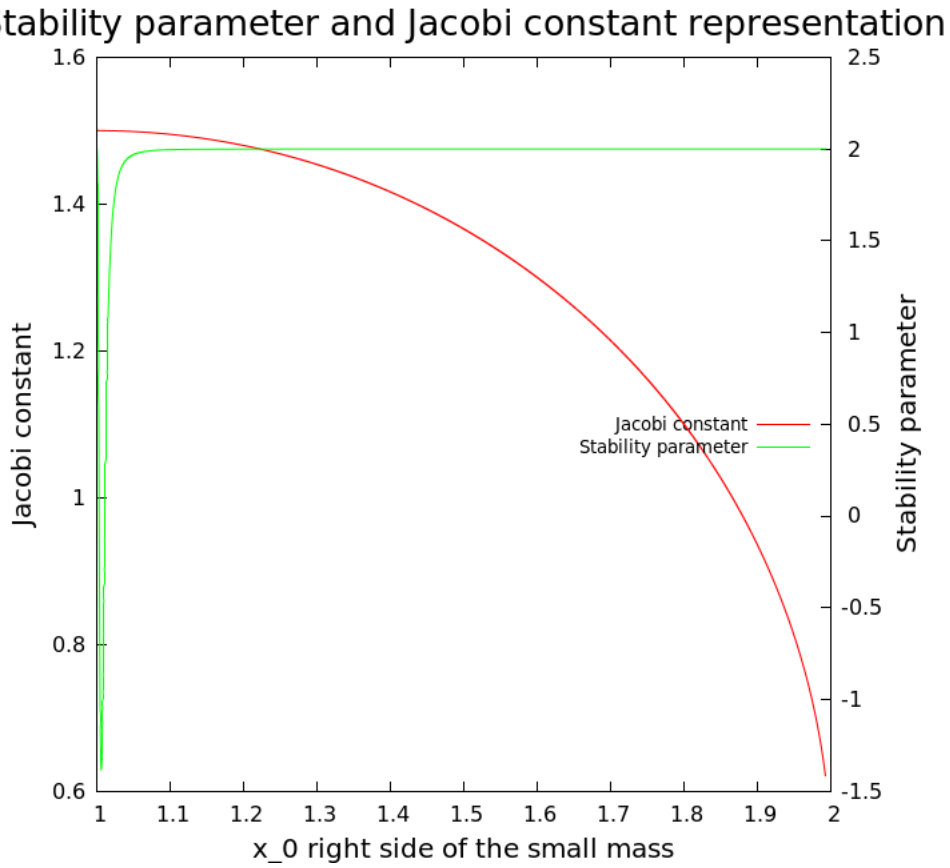

Figure 3.5: In this representation of the stability parameter of the retrograde orbits is seen that the orbits remain stable along the family, only having a small change in the stability parameter at the beginning of the family and being around $+2$ the most of the time. In order to read properly this figure it has to be read from left to right, because the orbits start from nearly $\xi_x \approx 1$. In this family, contrary to the family of direct orbits there is a bigger range in the Jacobi constant along the family. The starting orbit in this generation has been the same as in Figure 3.3.

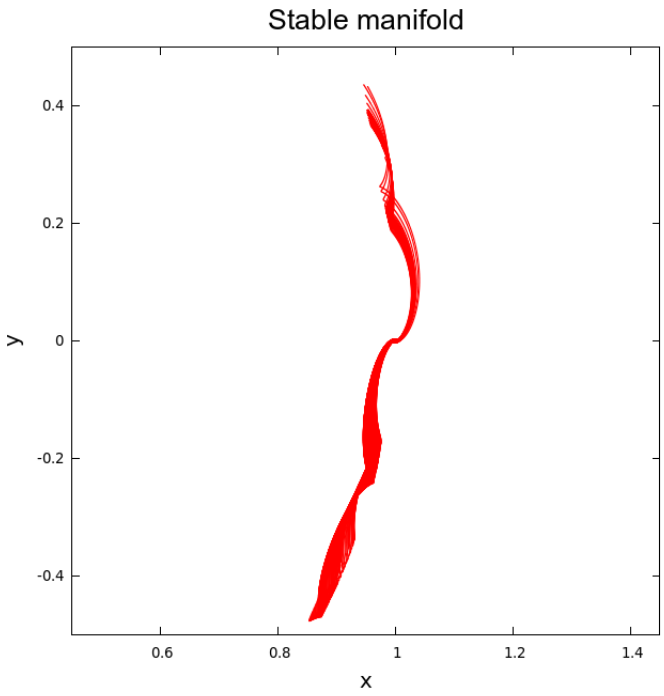

Figure 3.6: Computation of the stable manifold during about 20 units of time for $Tr = -150.28$.

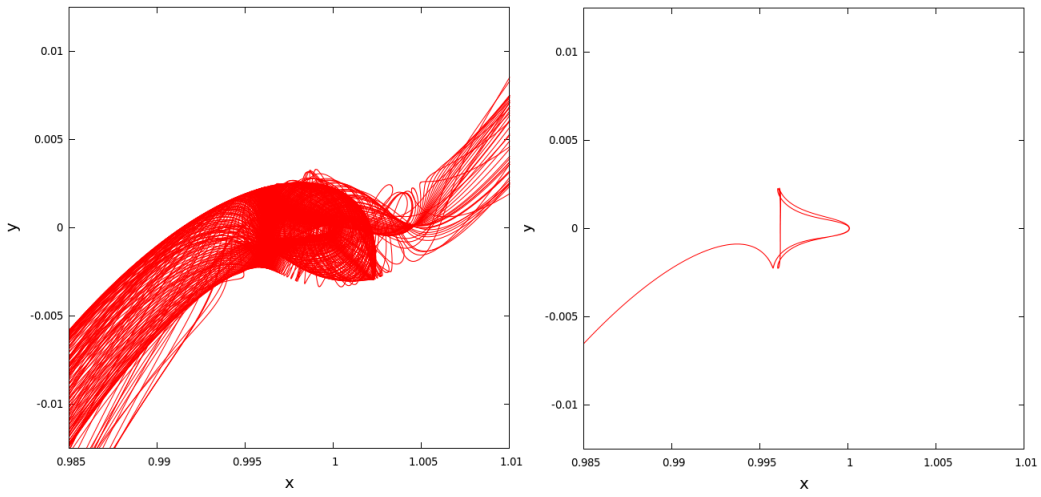

Figure 3.7: To the left a close-up of the stable manifold near the periodic orbit. To the right a single perturbed orbit. $Tr = -150.28$.

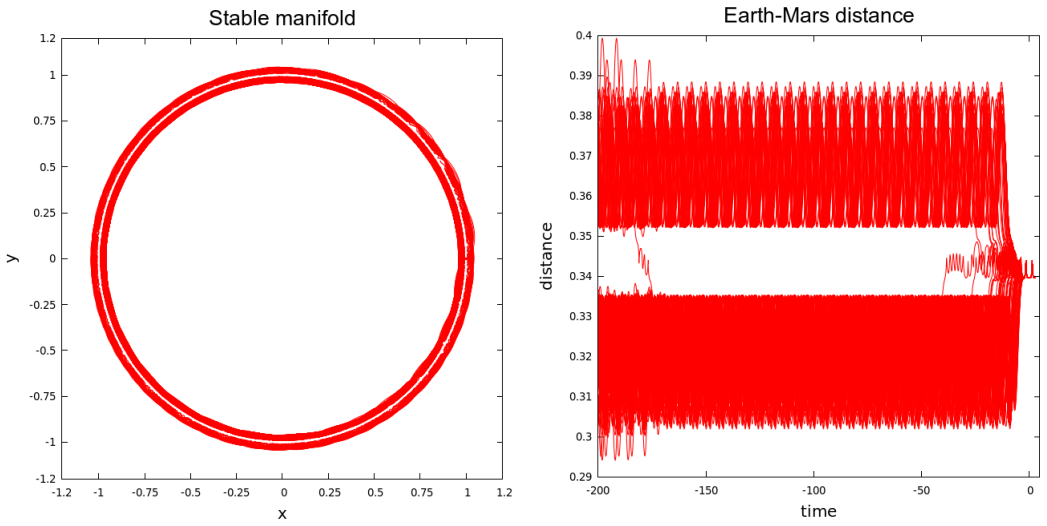

(a) Stable manifold for a sufficiently long time. (b) Distance from the stable manifold to the Earth.

Figure 3.8: Stable manifold and distance of this to the Earth for a stability parameter $Tr = -40.45$ and computed up to 200 units of time. It can be observed that the stable manifold is composed by two separated rings.

approximate Earth-Mars distance is $d_{E-M} \approx 0.343687$ and we want to obtain the distance from the Earth to the invariant manifold, let's say $d_{\mathcal{M}}$, and see how much smaller than d_{E-M} is.

There have been chosen for the study four different orbits with stability parameters $Tr = -7.95$, $Tr = -40.45$, $Tr = -150.28$, $Tr = -220.15$ respectively. It has been computed the stable manifold of each of these periodic orbits up to $t = 200$, which is about thirty Martian years. As it is shown in figure 3.8b the distance, $d_{\mathcal{M}}$ is almost the same until passed the 175 units of time. This smaller distance might be due to numerical error propagation, nonetheless, is not of our interest being such a small difference for such a great time. Then it has been reduced to the study of the first $t = 20$[1]. For this task let's define $r = \dfrac{d_{E-M} - d_{\mathcal{M}}}{d_{E-M}}$ as the gained distance percentage.

In the results of this minimum value of the distance presented in Table 3.1 can be seen that it is gained about a 12% and a 14%. However, as can be observed in figure 3.9 there are some oscillations in the $d_{\mathcal{M}}$, then if instead of the minimum distance in these 20 units of time it is considered the first great peak of the oscillations in distance it can be reduced the time significantly. Let's compare this distances and times with the ones in Table 3.2. It is observed that it is a significant descent of the time and really small difference in the distance.

[1]There might be values with $t > 20$, this is because of the propagation in order to find the eigenvalue. The perturbation has been performed in a time different from zero, greater than zero in fact, and then the backward integration has been done until $t = -20$.

Tr	t	$d_{\mathcal{M}}$	r (%)
-7.95	20.557	0.30219	12.07
-40.45	17.438	0.30113	12.38
-150.28	18.206	0.29893	13.02
-220.15	18.767	0.29649	13.73

Table 3.1: Minimum distances $d_{\mathcal{M}}$ in the first 20 units of time and its corresponding stability parameter, time and gained distance percentage.

Tr	t	$d_{\mathcal{M}}$	r (%)
-7.95	14.508	0.30227	12.05
-40.45	9.618	0.30223	12.06
-150.28	12.170	0.29900	13.00
-220.15	12.741	0.29655	13.72

Table 3.2: First considerable minimum distances $d_{\mathcal{M}}$ and its corresponding stability parameter, time and gained distance percentage.

Although it seems to have similar r values along the stability parameter a more exhaustively exploration should be done in order to find the optimum relation between t and r.

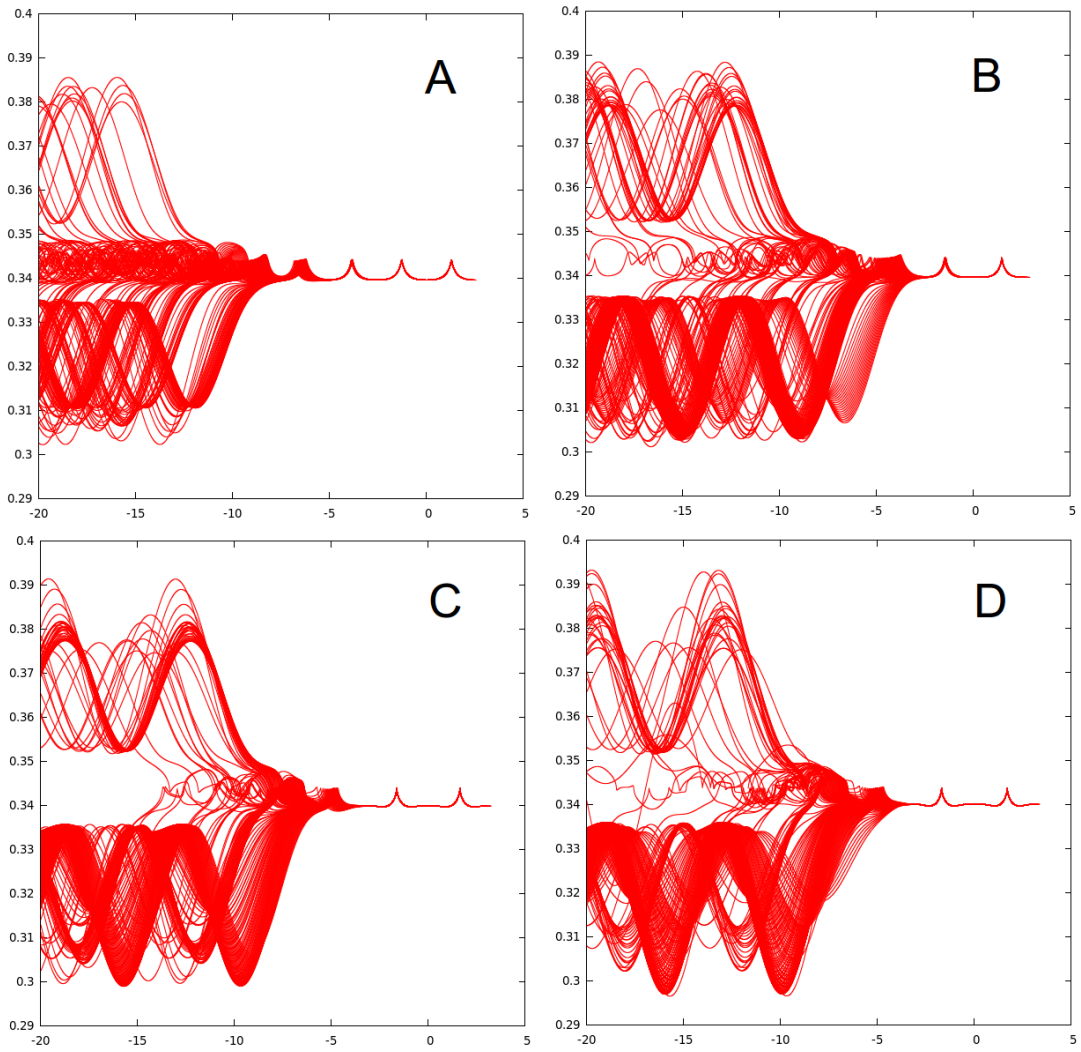

Figure 3.9: Distance from the stable manifold to the Earth for different stability parameters: A ($Tr = -7.95$), B ($Tr = -40.45$), C ($Tr = -150.28$), D ($Tr = -220.15$). In the A and B figures it has been applied a perturbation $\epsilon = 10^{-6}$ whereas in C and D it has been applied a perturbation of $\epsilon = 10^{-8}$.

Conclusions and further work

The main objective of this work, that was to explore if it is possible to find a transfer trajectory from the vicinity of the Earth to Mars using the stable manifold, has been satisfied and the answer, which was unknown, is negative. In the best case it has been reported a $r = 13.72\%$ which, although it represents about 7.5 million kilometres closer, it cannot be considered the vicinity of the Earth.

This project has provided the possibility to explore the subject of dynamical systems and its applications, a topic I am interested in. I have been able to familiarize with a range of different concepts, tools and methods as: the CR3BP; properties of the periodic orbits of the Hamiltonian systems; the invariant manifolds as tools of the study of dynamical systems; numerous numerical tools as integration of ODEs, the modified Newton method or the continuation of orbits along the family; and last but not least the application of the theoretical aspects to the resolution and computation of periodic orbits and its associated invariant manifolds.

I believe that the decision of redo or complementing the proofs from the references, or even state and prove propositions 2.20, 2.21 and 2.22 on my own, has been useful in the task of develop a more critical thinking and gain a deeper understanding of the theory. I am also happy with the justification of the methods of continuation and refinement, which in Simó, C. [9] the final results are almost directly exposed.

As a future work it would be interesting to introduce the gravitational effect of Jupiter as a periodic perturbation of the system, being this one the strongest affecting the the motion from the Earth to Mars, see Figure 3.10. It would be interesting to see how are perturbed the orbits around Mars, that will become quasi-periodic, as well as their stable manifold.

Another thing that would be interesting to do next is planning how to reach from the Earth the stable manifolds computed, taking into account that they do not come close to its vicinity. Perhaps a direct transfer to them using the Hohmann approach, with two impulsive manoeuvres one at the departure and the other at the arrival could be a first possibility. Another option is to use a low thrust transfer trajectory departing from the Earth until it reaches one of the orbits of the stable manifolds computed.

Although this method has seen not worthy for the problem of reaching Mars from the Earth, perhaps it would be a little bit more useful in another scenarios. In our first approach to the problem, in order to see if the computations were right, the software was applied to the Earth-Moon system, with a parameter $\mu = 1/82.27$, in order to compare results with Broucke, R. A. [11]. The stable manifold approach the primary significantly

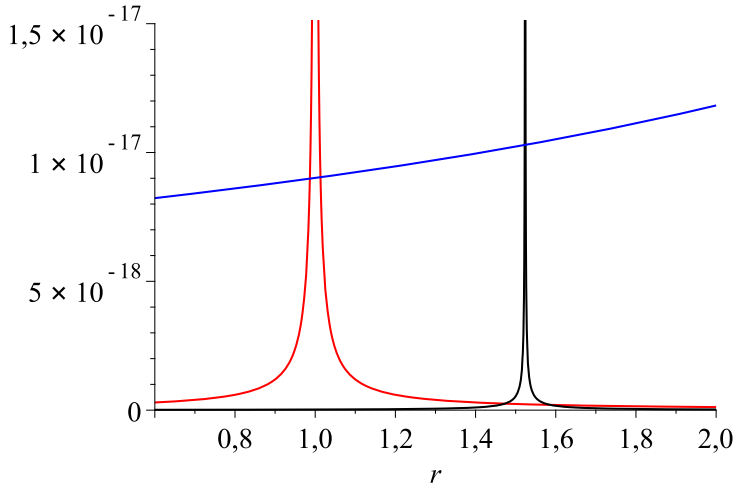

Figure 3.10: Gravity potential, in AU^2/s^2, of the Earth (red), Mars (black) and Jupiter (blue) as a function of the distance from the Sun, in astronomical units (AU).

more, that make us think that it might be a bit more useful if applied to systems with a bigger μ parameter as Sun-Jupiter, however, it probably still be not worthy because even if the stable manifold is closer to the Sun the distance between the Earth and Jupiter is also bigger.

Bibliography

[1] Szebehely, V. (1967). *Theory of orbits: The restricted problem of three bodies*. Academic Press.

[2] Meyer, K. Hall, G. (2009) *Introduction to Hamiltonian Dynamical Systems and the N-Body Problem*. Springer.

[3] Meyer, K. (1999) *Periodic Solutions of the N-Body Problem*. Berlin: Springer-Verlag.

[4] Siegel, C. L. and Moser, J. K. (1971) *Lectures on Celestial Mechanics*. Berlin: Springer-Verlag.

[5] Chicone, C. (1999) *Ordinary Differential Equations with Applications*. New York: Texts in Applied Mathematics 34, Springer.

[6] Palis, J. and de Melo, W. (1980) *Geometric Theory of Dynamical Systems*. New York: Springer-Verlag.

[7] Teschl, G. (2012) *Ordinary Differential Equations and Dynamical Systems*. American Mathematical Society.

[8] Gómez, G. Llibre, J. Martínez, R. and Simó, C. (2001) *Dynamics and Mission Design Near Libration Points. Vol. I Fundamentals: The Case of Collinear Libration Points*. Singapore: World Scientific Publishing Co. Pte. Ltd.

[9] Simó, C. (1990) *On the Analytical and Numerical Approximation of Invariant Manifolds*. Les Méthodes Modernes de la Mécanique Céleste. D. Benest, C. Froeschlé (eds.) pp 285-329.

[10] Saad, Y. (2011) *Numerical Methods for Large Eigenvalue Problems* Classics in Applied Mathematics, SIAM.

[11] Broucke, R. A. (1968) *Periodic Orbits in the Restricted Three-Body Problem With Earth-Moon Masses*. NASA Technical Report 32-1168. Jet Propulsion Laboratory, California Institute of Technology.

[12] E. Hairer, S. P. Norsett, G. Wanner. (2000) *Solving Ordinary Differential Equations I: Nonstiff Problems*. Berlin: Springer-Verlag